Journal of Medicinal Chemistry

Article

Cite This: J. Med. Chem. XXXX, XXX, XXX−XXX

pubs.acs.org/jmc

Aiming to Miss a Moving Target: Bromo and Extra Terminal Domain (BET) Selectivity in Constrained ATAD2 Inhibitors

Paul Bamborough,*[,†] Chun-wa Chung,[†] Rebecca C. Furze,[‡] Paola Grandi,[∥] Anne-Marie Michon,[∥] Robert J. Watson,[‡] Darren J. Mitchell,[‡] Heather Barnett,[§] Rab K. Prinjha,[‡] Christina Rau,[∥] Robert J. Sheppard,[‡,⊥] Thilo Werner,[∥] and Emmanuel H. Demont*[,‡]

[†]Molecular Discovery Research, [‡]Epigenetics Discovery Performance Unit, and [§]Flexible Discovery Unit, GlaxoSmithKline Medicines Research Centre, Gunnels Wood Road, Stevenage, Hertfordshire SG1 2NY, U.K.

[∥]Molecular Discovery Research, Cellzome GmbH, GlaxoSmithKline, Meyerhofstrasse 1, 69117 Heidelberg, Germany

Supporting Information

ABSTRACT: ATAD2 is a cancer-associated protein whose bromodomain has been described as among the least druggable of its class. In our recent disclosure of the first chemical probe against this bromodomain, GSK8814 (**6**), we described the use of a conformationally constrained methoxy piperidine to gain selectivity over the BET bromodomains. Here we describe an orthogonal conformational restriction strategy of the piperidine ring to give potent and selective tropane inhibitors and show structural insights into why this was more challenging than expected. Greater understanding of why different rational approaches succeeded or failed should help in the future design of selectivity in the bromodomain family.

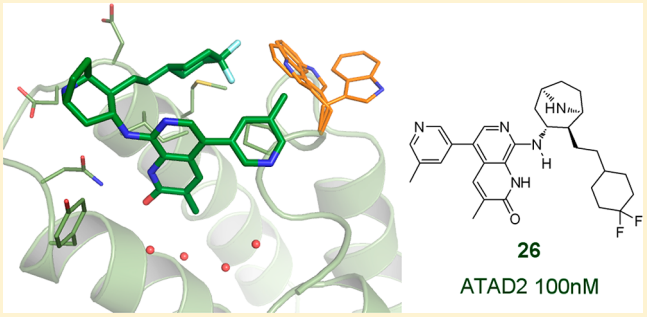

INTRODUCTION

ATAD2, also known as ATAD2A or ANCCA (AAA nuclear coregulator cancer-associated protein), is a nuclear protein normally expressed in germ cells and embryonic stem cells with a key role in chromatin remodelling.[1] Since its identification as a target gene in breast cancer,[2,3] ATAD2 has been shown to be highly expressed in a wide variety of unrelated cancers with increased expression levels correlating with disease recurrence and poor clinical prognosis.[4] Potential oncology indications include lung adenocarcinoma,[5] hepatocellular carcinoma,[6,7] colorectal,[8] ovarian,[9] and endometrial cancer[10] as well as osteosarcoma[11] and gastric cancer.[12]

As an oncology target, ATAD2 is supported by down-regulation of protein expression using siRNA technology. This has implicated the role of ATAD2 in pathways including apoptosis, cell survival, proliferation, and migration.[2,4,13−16] Mechanistically, ATAD2 has been shown to function as a coactivator for a variety of transcription factors including MYC, estrogen/androgen receptors, and E2F family members, directing transcription of a number of genes involved in cell proliferation and survival, including cyclins, Cdk2, and kinesins.[17−21] Furthermore, it has been demonstrated that ATAD2 is recruited to newly synthesized histones during DNA replication via a direct interaction with diacetylation modifications at K5 and K12 on histone H4.[22,23]

ATAD2 possesses a bromodomain and an ATPase associated with diverse cellular activities (AAA+) domain. So far, drug discovery efforts for oncology have focused on the ATAD2 bromodomain.[24,25] The discovery that molecules identified through phenotypic screens act by inhibition of the bromodomains of the BET family demonstrated the ligandability of bromodomains and highlighted their potential in a wide range of clinical indications, including oncology and inflammation.[26−28] A number of drug-like BET bromodomain inhibitors have now been reported, and over 20 clinical trials are underway studying their effects in oncology and inflammatory diseases.[29] A growing number of tool molecules have been reported to inhibit the bromodomains of non-BET proteins, including but not limited to CBP/EP300, BRD7/9, BRPF1, and SMARCA2/4.[30−32] Because of the potent pharmacology of even quite weak BET inhibitors,[33] cellular chemical probes of other bromodomains require exceptional selectivity. We have typically tried to reach 100−1000-fold selectivity. However, because of the conserved nature of bromodomain KAc sites, this is not always easily achieved. Greater understanding of which rational attempts to engineer greater selectivity succeed, and why they can unexpectedly fail, provides insights to inform future efforts.

We[34,35] and others[36−38] have identified small molecule inhibitors of the ATAD2/ATAD2B bromodomain to probe its functional role in disease and to assess if its inhibition was

Received: May 30, 2018

DOI: 10.1021/acs.jmedchem.8b00862
J. Med. Chem. XXXX, XXX, XXX−XXX

Table 1. Structure and Profile of Our Reported ATAD2 Inhibitors

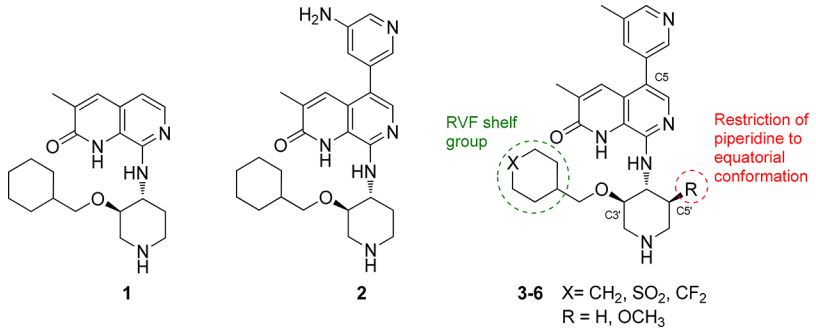

compd	R	X	ATAD2 pIC_{50}	BRD4 BD1 pIC_{50}	selectivity (fold)
1			5.6	5.4	2
2			6.9	6.2	5
3	H	CH_2	6.7	5.8	8
4	H	SO_2	6.9	4.8	125
5	OMe	SO_2	6.9	3.8	1300
6	OMe	CF_2	7.3	4.6	500

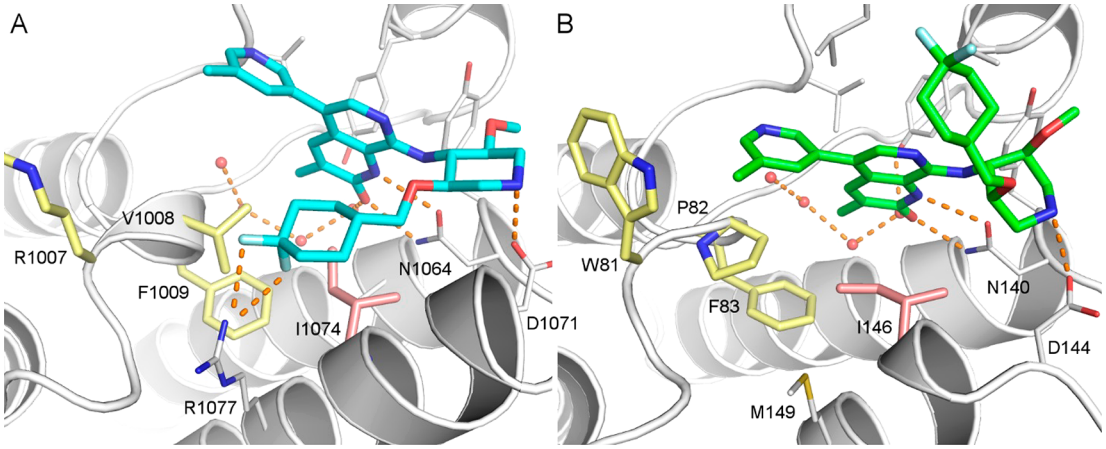

Figure 1. Compound **6** bound to ATAD2 and BRD4 (same orientation) illustrating the conformational basis for selectivity. In both proteins, the residues of the RVF/WPF motif are shown in pale yellow and the gatekeeper residue in salmon. In ATAD2 (A, PDB 5LJ0), the piperidine ring is triequatorial, positioning the C3′-substituent upon the RVF shelf where its CF_2 group interacts with R1077. In BRD4 (B, PDB 5LJ1), the triaxial piperidine geometry moves the C3′ substituent away from the WPF shelf into solvent.

sufficient to reproduce the promising results seen with siRNA knockdown. Starting from a fragment hit, we identified potent, cell permeable, highly selective ATAD2 inhibitors such as compound **6** (Table 1).[39] This uses a methoxy C5′-substituent to constrain the piperidine ring to an equatorial geometry in order to gain selectivity against the BET bromodomains. In this article, we present results from an alternative means of conformational restriction using 2-carbon-bridged piperidine (tropane) derivatives. This approach led to the identification of compounds with good potency and selectivity over the BET bromodomains. It also provided additional rationale for why compounds such as **6** have exceptional selectivity against BET.

As previously reported,[34,35] we used structure-based design to increase the potency and selectivity for ATAD2 over BRD4 BD1 (a representative of the eight bromodomains of this family, see Supporting Information, Tables S2 and S3) starting from compound **1** to give inhibitors such as **2** and **3** (Table 1). In particular we exploited the different interactions between the C3′-substituent and the RVF shelf in ATAD2 and the WPF shelf in BET. We reasoned that certain polar analogues of this cyclohexyl ring would interact better with the arginine side chains Arg1007 and Arg1077 found in ATAD2 than with the analogous tryptophan and methionine of the BET family (Trp81 and Met149 in BRD4 BD1), hence providing selectivity. This was indeed found to be the case (compare compounds such as **4** to **3**).[35] Crystal structures of the analogous quinolinone series in ATAD2 and BET revealed unexpected features of their binding modes.[39] In ATAD2, the piperidine lies in a trans-diequatorial conformation, making specific interactions with Arg1077. Unexpectedly, in BRD4 BD1 the piperidine ring adopts a trans-diaxial conformation to remove the polar sulfone C3′-group from the WPF shelf. Selectivity for ATAD2 over BRD4 BD1 was increased further by stabilizing the equatorial conformation versus the axial. This was achieved by the introduction of a C5′-methoxy substituent *cis* to the C3′ ether, giving **5**. This group creates a 1,3 steric strain in the putative triaxial conformation, disfavoring binding to BET, with limited impact on the triequatorial conformation seen in ATAD2. A final modification (isosteric substitution of the SO_2 group with CF_2) dramatically increased the passive permeability of our inhibitors, leading to compound **6** (GSK8814) the first potent, selective, and permeable

DOI: 10.1021/acs.jmedchem.8b00862
J. Med. Chem. XXXX, XXX, XXX−XXX

ATAD2 chemical probe.[40] Crystal structures of **6** showed that it also adopts a trans-equatorial conformation when bound to ATAD2 (Figure 1A) and a trans-triaxial conformation when bound to BRD4 BD1 (Figure 1B).

RESULTS AND DISCUSSION

While evaluating the impact of piperidine ring 1,3 sterics on BET selectivity, we also investigated other conformational constraints intended to force the shelf substituent into an equatorial position, including tropane derivatives. The starting points of this work were small analogues unsubstituted at the naphthyridone C5-position. As can be seen in Table 2, both

Table 2. Comparison of ATAD2 and BET Activity of Unfunctionalized Tropane and Piperidines

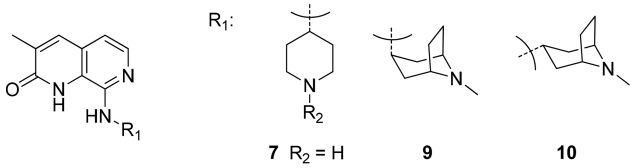

compd	ATAD2 pIC_{50}	BRD4 BD1 pIC_{50}
7	4.8	5.4
8	4.9	5.5
9	4.3	5.4
10	4.5	5.5

unsubstituted tropane isomers **9** and **10** have similar BET activity to the piperidine analogue **8**. Their potency against ATAD2 is slightly reduced, in particular for **9**, although this was not thought to be very significant.

Crystallographic data (Figure 2) showed that the tropane **10** has a similar ATAD2 binding mode to piperidine compounds such as **6**. We expected that the 3-pyridinyl substituents previously found to be advantageous at the naphthyridone C5-position could be incorporated directly into this new template. We also thought that the tropane could provide access to

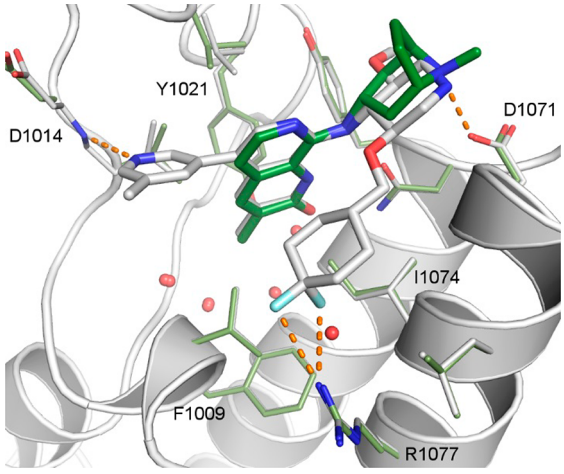

Figure 2. ATAD2 crystal structures of the NH piperidine GSK8814 (**6**, white, PDB 5LJ0) and the simplified tropane **10** (green, PDB 6HDN). Compound **6** uses its piperidine C3′-vector to make its CF_2 interaction with R1077, and its naphthyridone 5-position to make its pyridyl interaction with D1014. The analogous vectors are available to the tropane template **10**.

substitution vectors similar to the C5′-position of the piperidine of **6**. As a conformationally constrained alternative to the piperidine, the tropane could direct polar substituents onto the RVF shelf of ATAD2 and the WPF shelf of BET without permitting a conformational escape route and so exploit the differences between the amino acids there to gain selectivity.

The synthesis of functionalized tropanes is described in Scheme 1. The C3′-substituent was introduced via an aldol

Scheme 1. Synthetic Route to Functionalized Tropanes and Piperidines[a]

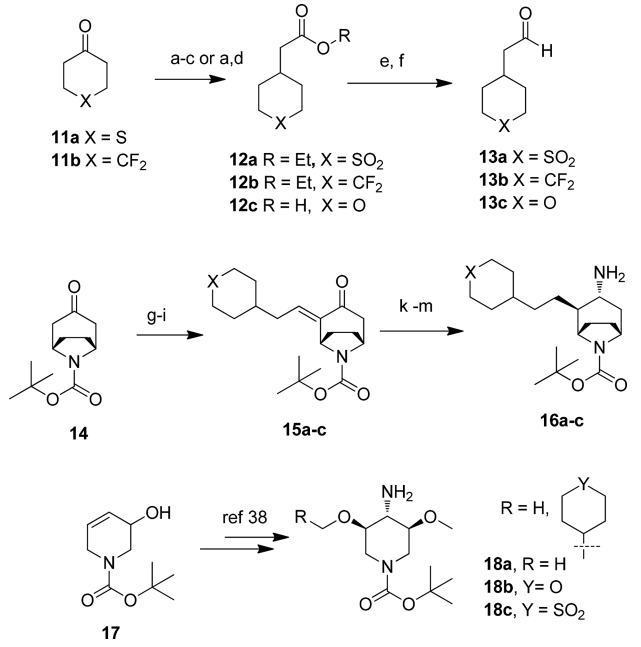

[a]Reagents and conditions: (a) $(Ph)_3P$ = CHCOOEt, toluene, 100 °C, 75−99%; (b) X = S, $NiCl_2$, $NaBH_4$, EtOH, 0 °C, 70%; (c) X = S, *m*-CPBA, CH_2Cl_2, 0 °C, 98%; (d) X = CF_2, H_2, Pd/C, MeOH, room temperature, 98%; (e) $LiAlH_4$, THF/Et_2O, −30 °C to room temperature, 88−100%; (f) $(COCl)_2$, DMSO, CH_2Cl_2, −78 °C then NEt_3; (g) LDA, THF, −78 °C then **13a**, **b**, or **c**; (h) $(CH_3SO_2)_2O$, NEt_3, CH_2Cl_2, 0 °C; (i) DBU, THF, room temperature, 69−70% over 4 steps; (j) H_2, Pd/C, MeOH/THF, room temperature, 74−79%; (k) NH_2OH.HCl, pyridine, EtOH, reflux, 89−100%; Na, EtOH, reflux, 47−76%.

reaction between ketone **14** and aldehydes **13a−c** (readily available from commercial ketones **11a,b** or acid **12c**). The intermediate alcohol was activated as a mesylate and eliminated to give alkenes **15a,c** as single stereoisomers in good yields. Following a stereoselective hydrogenation of the double bond, the ketone was converted to the oxime, which, on reduction with sodium metal, provided racemic amines **16a−c** as single diastereoisomers. We did not anticipate that changing the ether chain (as used in the piperidine series) to an alkyl chain (tropane series) to access the RVF shelf would have an impact as it did not have any in the piperidine series (see pairwise comparison in Figure S1, Supporting Information). The racemic synthesis of the analogous C3′−C5′ substituted derivatives **18a−c** from commercial **17** has already been described.[39]

These amines were then coupled to the known naphthyridone **19a**[35] (Scheme 2). The derivatives **20** were further functionalized at the C5 position following bromination and

DOI: 10.1021/acs.jmedchem.8b00862
J. Med. Chem. XXXX, XXX, XXX−XXX

Scheme 2. Synthesis of ATAD2 Inhibitors[a]

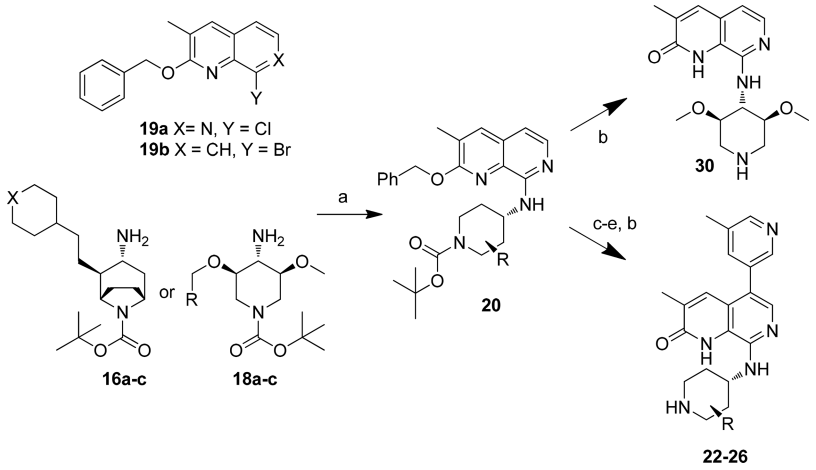

[a]Reagents and conditions: (a) *t*BuONa, BrettPhos, $Pd_2(dba)_3$, THF, 60 °C, 25−94%; (b) TFA, reflux, 63−96%; (c) NBS, CH_2Cl_2, 0 °C; (d) $ArB(OH)_2$, K_2CO_3, $Pd(OAc)_2$, di(1-adamantyl)-*n*-butylphosphine, 1,4-dioxane/water, 100 °C, 71−93% (2 steps); (e) chiral chromatography.

Suzuki coupling. Deprotection in acidic conditions gave the racemate of inhibitors **22**−**26**. The chiral separation of the racemic inhibitors or intermediates could be performed at any stage after the Buchwald coupling. In all cases, one enantiomer was significantly more potent at ATAD2 than the other. Co-crystallizations of the most active enantiomers in ATAD2 (or BRD4 BD1/BD2) always showed the same configuration, which is the one exemplified in all the schemes and tables. The analogous racemic quinolinone derivatives **27** and **28** (vide infra) could be obtained using the same sequence, starting from the known **19b** intermediate.[34] Compound **30** was obtained by direct deprotection of the corresponding intermediate **20**.

ATAD2 Activity of Tropane Derivatives. Table 3 compares activities against ATAD2 and BET for the mono- or disubstituted piperidines and their corresponding tropanes. These differ from **10** by the incorporation of substituents known to be favorable from our previous work, namely the methylpyridine at the naphthyridone C5-position and the introduction of tropane substituents intended to interact with the RVF shelf.[34,35] The combination of both modifications led to highly potent tropane-containing ATAD2 inhibitors such as **23**, **24**, and **26**, which also show excellent improvements in BET selectivity. The improvement in potency of these compounds over **10** is ∼100-fold, which is comparable to that found relative to **7** in the piperidine series.

Although we were unable to obtain a crystal structure of ATAD2 bound to **24**, we did manage to solve one in complex with its direct quinolinone N → CH analogue **27**. Figure 3 shows ATAD2 bound to **27** superimposed on our previously published structure of ATAD2 bound to **28**, which is the directly comparable quinolinone analogue of **4**.[35] In our

Table 3. Comparison of Activities between Tropane and Piperidine Derivatives

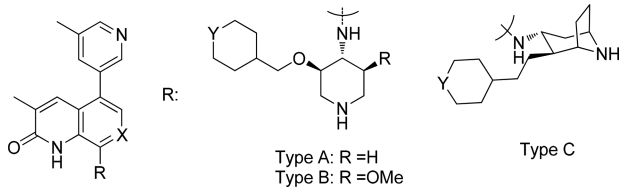

compd	X	type	Y	ATAD2 pIC_{50}	BRD4 BD1 pIC_{50}	selectivity (fold)
21	N	A	O	6.5	5.0	30
22	N	B		6.7	4.5	160
23	N	C		6.6	5.1	30
4	N	A	SO_2	6.9	4.8	125
5	N	B		6.9	3.8	1260
24	N	C		6.6	<4.3	>250
25	N	A	CF_2	7.4	5.2	150
6	N	B		7.3	4.6	500
26	N	C		7.0	5.3	60
27[a]	CH	C	SO_2	6.6	5.3	20
28[a]	CH	A		6.8	5.4	25

[a]Compounds are racemic.

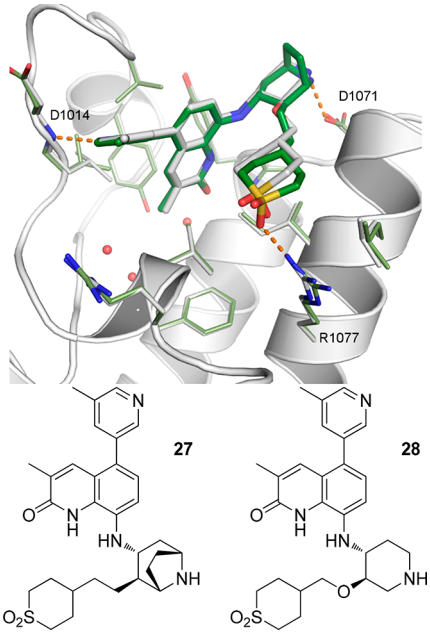

Figure 3. Superimposed crystal structures of the ATAD2-bound racemate of compound **27** (green, PDB 6HD0) and its direct piperidine analogue **28** (white, PBD 5A83).

DOI: 10.1021/acs.jmedchem.8b00862
J. Med. Chem. XXXX, XXX, XXX−XXX

previous work, we saw no structural differences in binding mode between the naphthyridone and quinolinone templates.[34] The ATAD2 binding mode of the substituted tropane derivative is very similar to its piperidine counterpart. Both derivatives form a hydrogen bond to Asp1071 via the piperidine or tropane nitrogen, anchoring this part of the molecule to the binding site. In the RVF shelf subpocket, a sulfone oxygen of each inhibitor is positioned appropriately to interact with Arg1077. In this particular example, the slight shift of the shelf substituent seen in the tropane series compared to the piperidine series might explain the minor decreases in ATAD2 potency observed for most pairs of examples made (Table 3, compare **24** to **4** and **5**).

The Selectivity of Constrained Tropane Derivatives over BRD4. From our previous work in the piperidine series, we understood that polar C3′-substituents (tetrahydropyran, difluoro-cyclohexyl, and cyclic sulfonamide) were favored on the RVF shelf of ATAD2 but poorly tolerated on the WPF shelf of BET.[35] Crystal structures showed that when these compounds bind to BRD4 BD1 their piperidine ring flips to adopt an axial conformation that allows the C3′-substituents to escape the WPF shelf environment by placing their polar functionality into solvent. Presumably this involves some conformational cost. Clearly, it would be impossible for the tropane derivatives to adopt this axial conformation.

The tropanes **23**, **24**, and **26** have fairly good BRD4 selectivity, comparable to or better than their monosubstituted piperidine analogues (**21**, **4**, and **25** respectively, Table 3). The selectivity for ATAD2 over BRD4 is most pronounced for the sulfone derivative **24** (>250-fold). This is approaching the selectivity window achieved by the trisubstituted methoxy-piperidine sulfone **5**. However, the THP and difluoro-cyclohexyl tropanes **23** and **26** did not quite achieve the level of selectivity reached by their direct methoxy-piperidine analogues **22** and **6**.

We used X-ray crystallography to investigate the reason why the BRD4 potency of tropane derivative **26** is around 5-fold greater than the disubstituted piperidine **6**. The X-ray structure of BRD4 BD1 bound to compound **26** is shown in Figure 4 compared to the previously published structure of BRD4 BD1 bound to **1** (PDB 5A85). The position of the naphthyridone core is not changed by the modifications. As expected, because of its constrained tropane ring, the difluorocyclohexane substituent of **26** is unable to move away from the WPF shelf of BRD4 unlike that of **6** (Figure 1B). The CF_2 group of **26** is forced to sit on the shelf in a region which is unfavorable due to steric or electrostatic interactions with Trp81. In this constrained situation, Trp81 responds to binding of **26** through a local rearrangement, adopting several different rotamers where the side chain moves away from the CF_2 group. These alternative conformers are rarely present in reported BRD4 BD1 structures in the Protein Data Bank (Figure S2, Supporting Information), but this increased disorder is apparently preferable to Trp81 remaining next to the difluorocyclohexane of the ligand. We attribute the lower BRD4 activity of the sulfone **24** relative to **26** to the adoption of a similar binding mode leaving the more polar SO_2 functionality in proximity to a rearranged Trp81.

In a further effort to understand better why the trisubstituted methoxy piperidines are more selective for ATAD2 over BRD4 BD1 than the tropanes, we made some simplified analogues lacking any C3′ substituents large enough to be able to occupy the WPF shelf (Table 4). The C3′−C5′ dimethoxy piperidine is intrinsically less active against BET (compare activity of compound **30** versus compounds **7**, **29**, or even **10**). The impact of C3′ and C5′ dimethoxy substitution on ATAD2 potency is much smaller than the impact on BET potency.

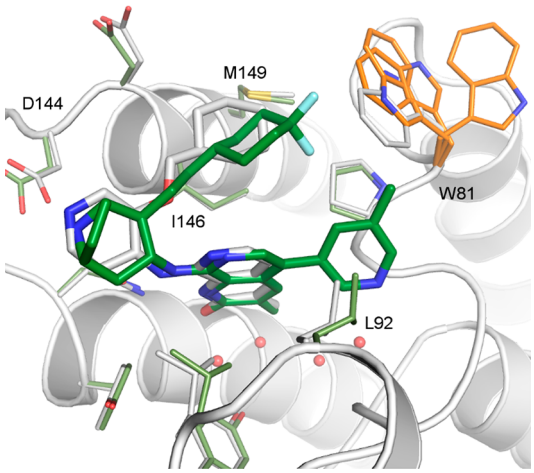

Figure 4. X-ray crystallographic binding mode of compound **26** (green, PDB 6HDQ) in BRD4 BD1, showing alternative conformers of Trp81 (orange). This is superimposed on the BRD4 structure of the racemate of **1** (white, PDB 5A85).

Table 4. Activity and Selectivity of Piperidine Bearing Small Substituents

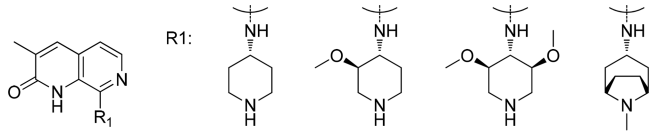

compd	ATAD2 pIC_{50}	BRD4 BD1 pIC_{50}
7	4.8	5.4
29	5.0	5.3
30	4.6	4.6
10	4.5	5.5

This can be understood by examining the crystal structures of **6** bound to ATAD2 and to BRD4 (Figure 5). The side chains of the ZA loop are closer to the inhibitor in BRD4 than ATAD2, leaving less space available at the piperidine C5′ position. The closest side chain of BRD4 to the C5′ atom of **25** in the crystal structure is Leu94 (3.8 Å distance). For comparison, in ATAD2 the closest side chain the C5′ atom of **6** is Val1018 (6.1 Å distance). Therefore, we conclude that in addition to the conformational contribution of the trisubstituted methoxypiperidine to the selectivity of **6** that we described previously, there also appears to be a steric component arising from the more limited amount of accessible space for the 5′-methoxy group in BRD4.

CONCLUSION

We set out to test the idea that constrained bridged piperidine derivatives would show greater selectivity over the BET bromodomains by rigidification, removing any possibility for the ligand to avoid placing polar C3′ substituents onto the WPF shelf. This led to the discovery of compounds such as **24** and **26** that are structurally different from our previous series.

DOI: 10.1021/acs.jmedchem.8b00862
J. Med. Chem. XXXX, XXX, XXX−XXX

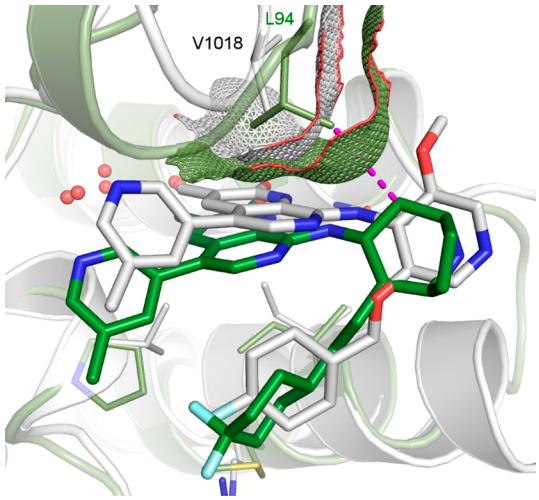

Figure 5. X-ray structures of ATAD2 bound to **6** (white, PDB 5LJ0) and BRD4 BD1 bound to **26** (green, PDB 6HDQ). The magenta dashed line shows the closest contact between **26** and BRD4 Leu94. Molecular surfaces of the closest side chains to the C3′-position (BRD4 Leu94 and ATAD2 Val1018) highlight the relatively greater space that is available for C3′ substituents in ATAD2 compared to BRD4.

These retain excellent ATAD2 potency and show good selectivity over BET.

The tropane derivatives were, however, less selective than their disubstituted piperidine analogues. Our efforts to understand the reasons for this led us to generate SAR with simplified compounds in the latter series, showing that dimethoxy substitution on the piperidine was intrinsically detrimental to BET activity. A closer examination of the crystal structures of this series bound to BRD4 and ATAD2 suggest that this is because the side chains of the ZA loop of BRD4 allow less space for substitution at the C5′ position. This further explains the exceptional selectivity seen with **6**.

The X-ray structure of the complex of BRD4 bound to **26** showed that the tropane does indeed force the difluorocyclohexyl substituent onto the WPF shelf. However, because this is electrostatically and/or sterically unfavorable, the crystal structure also revealed that as a result the protein undergoes an unexpected ligand-induced conformational change of the Trp81 side chain. This illustrates the complexity that can arise in interpreting the SAR of weak protein−ligand interactions and the difficulties that can complicate efforts to improve selectivity over an antitarget like BRD4. Rational modifications designed to introduce particular negative interactions to reduce binding affinity to the antitarget may be less effective than expected if the system can find ways to evade this interaction. Some systems, like BRD4, may find multiple ways to do this. In our earlier study on the piperidine series, we showed how the ligand escaped an unfavorable interaction with BRD4 Trp81 by adopting an unexpected axial conformational state, which limited the effectiveness of our rational design strategy until steps were taken to eliminate the unwanted conformer.[39] Here, we have shown that even when this escape route was blocked by rigidification of the ligand, the detrimental effects of the Trp81 interaction were still limited by an unanticipated conformational change, in this case, the ability of a side chain to move by adopting multiple rotameric states.

No doubt there are many cases where rational selectivity design has been attempted and found to be less successful than hoped, for similar reasons to those in our example. The explanation often remains poorly understood because crystallography of the antitargets may not be available or because crystallization of ligands that bind relatively weakly is challenging. However, when successful the structural insights may reveal unexpected ways that proteins or ligands can adapt to minimize unfavorable interactions, and this information can suggest new strategies to improve selectivity.

EXPERIMENTAL SECTION

Protein Expression, ATAD2 and BET Bromodomain Assays, and Physicochemical Property Measurement. These were carried out as described previously.[35]

Chemistry. All solvents were purchased from Sigma-Aldrich (Hy-Dry anhydrous solvents) and commercially available reagents were used as received. All reactions were followed by TLC analysis (TLC plates GF254, Merck) or liquid chromatography mass spectrometry (LCMS) using a Waters ZQ instrument. NMR spectra were recorded on a Bruker nanobay 400 MHz or a Bruker AVII+ 600 MHz spectrometers and are referenced as follows: ^{1}H NMR (400 or 600 MHz), internal standard TMS at δ = 0.00. ^{13}C NMR (100.6 or 150.9 MHz), internal standard $CDCl_3$ at δ = 77.23 or DMSO-d_6 at δ = 39.70. Column chromatography was performed on prepacked silica gel columns (30−90 mesh, IST) using a biotage SP4. Mass spectra were recorded on Waters ZQ (ESI-MS) and Q-Tof 2 (HRMS) spectrometers. Mass directed auto prep was performed on a Waters 2767 with a MicroMass ZQ mass spectrometer using a Supelco LCABZ++ column.

Synthetic Methods and Characterization of Compounds. Abbreviations for multiplicities observed in NMR spectra: s; singulet; br s, broad singulet; d, doublet; t, triplet; q, quadruplet; p, pentuplet; spt, septuplet; m, multiplet. The purity of all compounds was determined by LCMS and ^{1}H NMR and was always >95%.

LCMS. UPLC analysis was conducted on an Acquity UPLC BEH C18 column (50 mm × 2.1 mm, i.d. 1.7 μm packing diameter) at 40 °C. Formate method: solvents employed were A = 0.1% v/v solution of formic acid in water; B = 0.1% v/v solution of formic acid in acetonitrile. High pH method: the solvents employed were: A = 10 mM ammonium hydrogen carbonate in water adjusted to pH 10 with ammonia solution; B = acetonitrile. For both methods, the gradient employed was (Table 5):

Table 5

time (min)	flow rate (mL/min)	%A	%B
0	1	99	1
1.5	1	3	97
1.9	1	3	97
2.0	1	0	100

The UV detection was a summed signal from wavelength of 210 to 350 nm. Mass spectra were obtained on a Waters ZQ instrument; ionization mode, alternate-scan positive, and negative electrospray; scan range 100 to 1000 AMU; scan time 0.27 s; interscan delay 0.10 s.

MDAP. Formate method: HPLC analysis was conducted on either a Sunfire C18 column (100 mm × 19 mm, i.d 5 μm packing diameter) or a Sunfire C18 column (150 mm × 30 mm, i.d. 5 μm packing diameter) at ambient temperature. The solvents employed were: A = 0.1% v/v solution of formic acid in water; B = 0.1% v/v solution of formic acid in acetonitrile. Run as a gradient over either 15 or 25 min (extended run) with a flow rate of 20 mL/min (100 mm × 19 mm, i.d. 5 μm packing diameter) or 40 mL/min (150 mm × 30 mm, i.d. 5 μm packing diameter). High pH method: HPLC analysis was conducted on either an Xbridge C18 column (100 mm × 19 mm, i.d. 5 μm packing diameter) or a Xbridge C18 column (100 mm × 30 mm, i.d. 5 μm packing diameter) at ambient temperature. The solvents employed were: A = 10 mM ammonium bicarbonate in water, adjusted to pH10 with ammonia solution; B = acetonitrile. Run

DOI: 10.1021/acs.jmedchem.8b00862
J. Med. Chem. XXXX, XXX, XXX−XXX

as a gradient over either 15 or 25 min (extended run) with a flow rate of 20 mL/min (100 mm × 19 mm, i.d. 5 μm packing diameter) or 40 mL/min (100 mm × 30 mm, i.d. 5 μm packing diameter). For both methods, the UV detection was a summed signal from wavelength of 210−350 nm. Mass spectra were obtained on a Waters ZQ instrument; ionization mode, alternate-scan positive, and negative electrospray; scan range 100−1000 AMU; scan time 0.50 s; interscan delay 0.20 s.

Compounds **1**−**10**, **19a,b**, **21**, **25**, and **29** synthesis have already been published.[33,34,38]

Ethyl 2-(1,1-Dioxidotetrahydro-2*H*-thiopyran-4-yl)acetate (12a). Step 1: A solution of dihydro-2*H*-thiopyran-4(3*H*)-one (11.45 g, 99.00 mmol) and ethyl 2-(triphenylphosphoranylidene)-acetate (36.0 g, 103 mmol) in toluene (300 mL) was stirred at 100 °C for 8 h. Ethyl 2-(triphenylphosphoranylidene)acetate (4.0 g, 11 mmol) was added, and the mixture was stirred for another 4 h and then was cooled to room temperature. The solvent was removed in vacuo, and the residue was triturated with Et_2O. The solid Ph_3PO formed was filtered off and rinsed with Et_2O, and the combined organics were concentrated in vacuo. Purification of the residue by flash chromatography on silica gel (340 g column, 10% GLOBAL gradient (AcOEt in hexanes)) gave ethyl 2-(dihydro-2*H*-thiopyran-4(3*H*)-ylidene)acetate (13.7 g, 75%) as colorless oil. ^{1}H NMR (400 MHz, $CDCl_3$) δ ppm 5.69 (s, 1H), 4.16 (q, J = 7.2 Hz, 2H), 3.21 (m, 2H), 2.82−2.73 (m, 4H), 2.59−2.50 (m, 2H), 1.29 (t, J = 7.2 Hz, 3H). Step 2: A solution of ethyl 2-(dihydro-2*H*-thiopyran-4(3*H*)-ylidene)acetate (7.88 g, 42.3 mmol) in EtOH (160 mL) at 0 °C was treated with nickel(II) chloride (16.4 g, 127 mmol) then with sodium borohydride (6.40 g, 169 mmol) Portionwise (1 g every 10 min). Then 2 h after the final addition, the solvent was removed in vacuo and the residue was partitioned between EtOAc and water. The biphasic phase was filtered through Celite and the layers were separated. The aqueous phase was extracted twice with EtOAc, and the combined organics were washed twice with brine, dried over $MgSO_4$, and concentrated in vacuo to give ethyl 2-(tetrahydro-2*H*-thiopyran-4-yl)acetate (5.6 g, 70%) as a colorless oil, which was used in the next step without further purification. ^{1}H NMR (400 MHz, $CDCl_3$) δ 4.17 (q, J = 7.1 Hz, 2H), 3.10−2.97 (m, 4H), 2.34 (d, J = 6.6 Hz, 2H), 2.21−2.05 (m, 3H), 2.02−1.85 (m, 2H), 1.28 (t, J = 7.1 Hz, 3H). Step 3: A solution of ethyl 2-(tetrahydro-2*H*-thiopyran-4-yl)acetate (5.6 g, 30 mmol) in CH_2Cl_2 (150 mL) at 0 °C was treated with m-CPBA (<77% w/w, 12.7 g, 62.5 mmol) in two portions, and the resulting mixture was stirred at this temperature. After 30 min, CH_2Cl_2 (150 mL) was added to help stirring. After 6 h, the mixture was treated with sodium thiosulfate (9.40 g, 59.5 mmol) in water (50 mL). The mixture was vigorously stirred for 10 min, and the layers were separated. The aqueous phase was extracted with CH_2Cl_2, and the combined organic phases were washed three times with a saturated $NaHCO_3$ aqueous solution, dried using a phase separator, and concentrated in vacuo to give ethyl 2-(1,1-dioxidotetrahydro-2*H*-thiopyran-4-yl)acetate (**12a**) (6.43 g, 98%) as a white solid which was used in the next step without further purification. ^{1}H NMR (400 MHz, $CDCl_3$) δ 4.16 (q, J = 7.1 Hz, 2H), 3.10−2.93 (m, 4H), 2.34 (d, J = 6.8 Hz, 2H), 2.19−2.04 (m, 2H), 2.00−1.85 (m, 2H), 1.78−1.72 (m, 1H), 1.28 (t, J = 7.1 Hz, 3H).

Ethyl 2-(4,4-Difluorocyclohexyl)acetate (12b). Step 1: A solution of 4,4-difluorocyclohexanone (7.35 g, 54.8 mmol) and ethyl 2-(triphenylphosphoranylidene)acetate (21.0 g, 60.3 mmol) in toluene (100 mL) was stirred at 100 °C for 16 h then was cooled to room temperature and concentrated in vacuo. The residue was triturated with Et_2O and the solid formed (Ph_3PO) removed by filtration and rinsed with Et_2O. The combined organics were concentrated in vacuo. Purification of the residue obtained by flash chromatography on silica gel (340 g column, 10% GLOBAL gradient (AcOEt in hexanes)) gave ethyl 2-(4,4-difluorocyclohexylidene)-acetate (11.0 g, 99%) as a colorless oil. ^{1}H NMR (400 MHz, $CDCl_3$) δ 5.75 (s, 1H), 4.18 (q, J = 7.1 Hz, 2H), 3.10−3.01 (m, 2H), 2.46−2.37 (m, 2H), 2.13−1.96 (m, 4H), 1.30 (t, J = 7.1 Hz, 3H). Step 2: A solution of ethyl 2-(4,4-difluorocyclohexylidene)acetate (11.0 g, 54.0 mmol) in MeOH (160 mL) at room temperature was treated with palladium on carbon (10% w/w, 50% wet, 1 g), and the resulting mixture was stirred under an atmosphere of hydrogen (1 bar) for 16 h. The catalyst was removed using a pad of Celite (10 g) and rinsed with EtOAc. The combined organics were concentrated in vacuo to give ethyl 2-(4,4-difluorocyclohexyl)acetate (**12b**) (10.94 g, 98%) as a colorless oil which was used in the next step without further purification. ^{1}H NMR (400 MHz, $CDCl_3$) δ 4.16 (q, J = 7.1 Hz, 2H), 2.26 (d, J = 7.1 Hz, 2H), 2.16−2.04 (m, 2H), 1.97−1.66 (m, 5H), 1.42−1.31 (m, 2H), 1.28 (t, J = 7.1 Hz, 3H).

2-(1,1-Dioxidotetrahydro-2*H*-thiopyran-4-yl)acetaldehyde (13a). Step 1: A solution of ethyl 2-(1,1-dioxidotetrahydro-2*H*-thiopyran-4-yl)acetate (**12a**) (6.42 g, 29.1 mmol) in THF (150 mL) under nitrogen at −30 °C was treated with $LiAlH_4$ (1 M in Et_2O, 29.1 mL, 29.1 mmol), and the resulting mixture was stirred for 1.5 h between −30 °C and −20 °C. The mixture was then carefully treated with water (0.960 mL, 1 mL/g $LiAlH_4$), then with 15% w/w NaOH in water (0.960 mL), and then with 3 times 0.960 mL of water. The corresponding mixture was stirred at room temperature for 10 min. The white precipitate formed was filtered through a 2.5 g pad of Celite and rinsed with THF. The combined organics were concentrated in vacuo to give 4-(2-hydroxyethyl)tetrahydro-2*H*-thiopyran 1,1-dioxide (5.51 g, 106%) as a colorless oil which was used in the next step without further purification. ^{1}H NMR (400 MHz, $CDCl_3$) δ 3.80−3.67 (m, 2H), 3.13−2.93 (m, 4H), 2.15 (m, 2H), 1.97−1.50 (m, 6H). Step 2: A solution of oxalyl chloride (2.27 mL, 26.0 mmol) in CH_2Cl_2 (100 mL) at −78 °C under nitrogen was treated with DMSO (2.83 mL, 39.9 mmol) in CH_2Cl_2 (5 mL) dropwise, and the resulting mixture was stirred at this temperature for 15 min before being treated with 4-(2-hydroxyethyl)tetrahydro-2*H*-thiopyran 1,1-dioxide (3.56 g, 20.0 mmol) in CH_2Cl_2 (15 mL plus 2 mL rinse). The resulting mixture was stirred for 30 min at this temperature before being treated with NEt_3 (8.35 mL, 59.9 mmol). The resulting mixture was stirred at this temperature for 30 min then was warmed to room temperature and stirred for 30 min before being diluted with CH_2Cl_2. The organic phase was washed with water, and the aqueous phase was extracted with CH_2Cl_2. The combined organics were dried using a phase separator and concentrated in vacuo to give 2-(1,1-dioxidotetrahydro-2*H*-thiopyran-4-yl)acetaldehyde (**13a**) (3.52 g, 100%) as a white solid which was used in the next step without further purification. ^{1}H NMR (400 MHz, $CDCl_3$) δ 9.77 (br s, 1H), 3.07−2.99 (m, 4H), 2.52 (dd, J = 6.6, 1.0 Hz, 2H), 2.28−2.16 (m, 1H), 2.16−2.05 (m, 2H), 1.99−1.81 (m, 2H).

2-(4,4-Difluorocyclohexyl)acetaldehyde (13b). Step 1: A solution of ethyl 2-(4,4-difluorocyclohexyl)acetate (**12b**) (10.5 g, 50.9 mmol) in THF (300 mL) under nitrogen at −30 °C was treated with $LiAlH_4$ (2 M in Et_2O, 25.5 mL, 51.0 mmol), and the resulting mixture was stirred for 1.5 h between −30 and −20 °C then was carefully treated with water (1.9 mL, 1 mL/g LaH) then 1.9 mL of a 15% w/w NaOH in water then with 3 × 1.9 mL of water. The corresponding mixture was stirred at room temperature for 10 min, then the white precipitate formed was filtered through Celite (2.5 g pad) and rinsed with THF. The combined organics were concentrated in vacuo to give 2-(4,4-difluorocyclohexyl)ethanol (7.34 g, 88%) as a colorless oil which was used in the next step without further purification. ^{1}H NMR (400 MHz, $CDCl_3$) δ 3.77−3.63 (m, 2H), 2.15−2.01 (m, 2H), 1.89−1.62 (m, 5H), 1.59−1.46 (m, 3H), 1.39−1.20 (m, 2H). Step 2: A solution of oxalyl chloride (5.87 mL, 67.1 mmol) in CH_2Cl_2 (250 mL) at −78 °C under nitrogen was treated with DMSO (7.93 mL, 112 mmol) in CH_2Cl_2 (10 mL) dropwise, and the resulting mixture was stirred at this temperature for 20 min before being treated with 2-(4,4-difluorocyclohexyl)ethanol (7.34 g, 44.7 mmol) in CH_2Cl_2 (20 mL + 2 mL rinse). The resulting mixture was stirred for 30 min at this temperature before being treated with triethylamine (19.9 mL, 143 mmol). The resulting mixture was stirred at this temperature for 1 h, then was warmed to room temperature, stirred 20 min, and diluted with CH_2Cl_2. The organic phase was washed with water, and the aqueous phase was extracted with CH_2Cl_2. The combined organics were washed with water/brine 1:1, dried using a phase separator, and concentrated in vacuo to give 2-(4,4-difluorocyclohexyl)acetaldehyde

DOI: 10.1021/acs.jmedchem.8b00862
J. Med. Chem. XXXX, XXX, XXX−XXX

(**13b**) (7.5 g, assumed quantitative) as a yellow solid which was used in the next step without further purification. ^{1}H NMR (400 MHz, $CDCl_3$) δ 9.80 (t, J = 1.6 Hz, 1H), 2.43 (dd, J = 6.8, 1.6, Hz, 2H), 2.17−1.95 (m, 2H), 2.04−1.95 (m, 1H), 1.87−1.78 (m, 3H), 1.78−1.66 (m, 1H), 1.43−1.29 (m, 2H).

2-(Tetrahydro-2*H*-pyran-4-yl)acetaldehyde (13c). Step 1: A solution of 2-(tetrahydro-2*H*-pyran-4-yl)acetic acid (**12c**) (5.00 g, 34.7 mmol) in THF (100 mL) at 0 °C under nitrogen was slowly treated with $LiAlH_4$ (1 M in THF, 34.7 mL, 34.7 mmol). The mixture was then allowed to warm to room temperature and was stirred for 24 h. The mixture was then cooled to 0 °C and carefully treated with water (1.3 mL, 1 mL/g $LiAlH_4$) then with 1.3 mL of 15% w/w NaOH in water then with 3 × 1.3 mL of water. The resulting mixture was stirred at room temperature for 10 min, then the white precipitate formed was filtered through a pad of Celite (2.5 g) and rinsed with EtOAc. The combined organic phases were concentrated in vacuo. The residue was dissolved in CH_2Cl_2, and the organic phase was dried using a phase separator and concentrated in vacuo to give 2-(tetrahydro-2*H*-pyran-4-yl)ethanol (4.28 g, 95%) as a very pale-yellow oil which was used in the next step without further purification. ^{1}H NMR (400 MHz, $CDCl_3$) δ 3.96 (dd, J = 11.1 4.0 Hz, 2H), 3.78−3.65 (m, 2H), 3.40 (t, J = 11.7 Hz, 2H), 1.79−1.24 (m, 8H). Step 2: A solution of oxalyl chloride (4.29 mL, 49.0 mmol) in CH_2Cl_2 (100 mL) under nitrogen was cooled to −78 °C then treated with DMSO (5.8 mL, 82 mmol) in CH_2Cl_2 (15 mL) dropwise. The resulting mixture was stirred for 15 min at this temperature before being treated with 2-(tetrahydro-2*H*-pyran-4-yl)ethanol (4.25 g, 32.6 mmol) in CH_2Cl_2 (20 mL). The resulting mixture was stirred at this temperature for 30 min before being treated with NEt_3 (14.6 mL, 104 mmol) . The resulting mixture was stirred at this temperature for 1 h then was warmed to room temperature and diluted with CH_2Cl_2 after 20 min. The organic phase was washed with water (which was then extracted with CH_2Cl_2), and the combined organics were washed with water again, dried using a phase separator, and concentrated in vacuo to give crude 2-(tetrahydro-2*H*-pyran-4-yl)acetaldehyde (**13c**) (5 g, assumed quantitative) as a pale-yellow oil which was used in the next step without further purification. ^{1}H NMR (400 MHz, $CDCl_3$) δ 9.79 (t, J = 1.7 Hz, 1H), 3.99−3.92 (m, 2H), 3.44 (dt, J = 11.8, 2.1 Hz, 2H), 2.40 (dd, J = 6.7, 1.8, Hz, 2H), 2.24−2.08 (m, 1H), 1.69−1.59 (m, 2H), 1.44−1.30 (m, 2H).

(*E*)-*tert*-Butyl 2-(2-(1,1-Dioxidotetrahydro-2*H*-thiopyran-4-yl)ethylidene)-3-oxo-8-azabicyclo[3.2.1]octane-8-carboxylate (15a). Step 1: A solution of diisopropylamine (3.98 mL, 28.0 mmol) in THF (100 mL) at −78 °C under nitrogen was treated with *n*-butyllithium (1.6 M in hexanes, 16.2 mL, 26.0 mmol) dropwise. After 5 min, the mixture was warmed to 0 °C using an ice bath, stirred 30 min at this temperature, and then cooled again at −78 °C. The mixture was then treated with *tert*-butyl 3-oxo-8-azabicyclo[3.2.1]-octane-8-carboxylate (**14**) (5.40 g, 24.0 mmol) in THF (25 mL plus 5 mL rinse). The resulting mixture was stirred for 1 h at this temperature before being treated with 2-(1,1-dioxidotetrahydro-2*H*-thiopyran-4-yl)acetaldehyde (**13a**) (3.52 g, 20.0 mmol) in THF (10 mL plus 2 mL rinse). The resulting mixture was stirred for 2 h at −78 °C then was treated with a saturated NH_4Cl aqueous solution. The mixture was warmed to room temperature and diluted with EtOAc and water. The layers were separated. The aqueous phase was extracted with EtOAc, and the combined organics were washed with brine, dried over $MgSO_4$, and concentrated in vacuo to give crude *tert*-butyl 2-(2-(1,1-dioxidotetrahydro-2*H*-thiopyran-4-yl)-1-hydroxyethyl)-3-oxo-8-azabicyclo[3.2.1]octane-8-carboxylate (9.0 g, 112%) as a pale-yellow solid which was used in the next step without further purification. Step 2: A solution of crude *tert*-butyl 2-(2-(1,1-dioxidotetrahydro-2*H*-thiopyran-4-yl)-1-hydroxyethyl)-3-oxo-8-azabicyclo[3.2.1]octane-8-carboxylate (9.0 g, 20 mmol) in CH_2Cl_2 (100 mL) at 0 °C under nitrogen was treated with NEt_3 (5.57 mL, 39.9 mmol) then methanesulfonic anhydride (3.83 g, 22.0 mmol) and the resulting mixture was stirred at this temperature for 40 min and then was washed with water. The aqueous phase was extracted with CH_2Cl_2 and the combined organics were dried using a phase separator and concentrated in vacuo to give crude *tert*-butyl 2-(2-(1,1-dioxidotetrahydro-2*H*-thiopyran-4-yl)-1-((methylsulfonyl)oxy)ethyl)-3-oxo-8-azabicyclo[3.2.1]octane-8-carboxylate (9.58 g, 100%) as a white foam which was used in the next step without further purification. Step 3: A solution of crude *tert*-butyl 2-(2-(1,1-dioxidotetrahydro-2*H*-thiopyran-4-yl)-1-((methylsulfonyl)oxy)ethyl)-3-oxo-8-azabicyclo[3.2.1]octane-8-carboxylate (9.58 g, 20.0 mmol) in THF (100 mL) at room temperature was treated with DBU (6.02 mL, 39.9 mmol), and the resulting mixture was stirred at this temperature for 30 min then most of the solvent was evaporated in vacuo. The residue was partitioned between EtOAc and water, and the layers were separated. The aqueous phase was extracted twice with EtOAc, and the combined organics were washed with brine, dried over $MgSO_4$, and concentrated in vacuo to give a yellow solid. Trituration of this residue with methanol gave (*E*)-*tert*-butyl 2-(2-(1,1-dioxidotetrahydro-2*H*-thiopyran-4-yl)ethylidene)-3-oxo-8-azabicyclo-[3.2.1]octane-8-carboxylate (**15a**) (4.11 g, 54%) as a white solid. The mother liquors were concentrated in vacuo. Purification of the residue obtained by flash chromatography on silica gel (100 g column, 50% GLOBAL gradient (AcOEt in hexanes)) gave (*E*)-*tert*-butyl 2-(2-(1,1-dioxidotetrahydro-2*H*-thiopyran-4-yl)ethylidene)-3-oxo-8-azabicyclo-[3.2.1]octane-8-carboxylate (**15a**) (1.18 g, 15%) as a white solid after trituration with MeOH. Overall yield of 69% over 4 steps. The stereochemistry of the alkene was confirmed by NMR. LCMS (method high pH): Retention time 0.93 min, $[M + H]^+$ = 384.3. ^{1}H NMR (600 MHz, DMSO-d_6) δ 6.36 (t, J = 7.9 Hz, 1H), 5.01 (d, J = 6.0 Hz, 1H), 4.33 (dd, J = 6.0, 4.5 Hz, 1H), 3.15−3.07 (m, 2H), 3.04−2.97 (m, 2H), 2.63 (dd, J = 18.0, 4.5 Hz, 1H), 2.38 (d, J = 18.3 Hz, 1H), 2.25−2.18 (m, 2H), 2.18−2.09 (m, 2H), 1.96 (d, J = 13.9 Hz, 2H), 1.85−1.76 (m, 1H), 1.71−1.61 (m, 3H), 1.61−1.53 (m, 1H), 1.38 (s, 9H).

(*E*)-*tert*-Butyl 2-(2-(4,4-Difluorocyclohexyl)ethylidene)-3-oxo-8-azabicyclo[3.2.1]octane-8-carboxylate (15b). Step 1: A solution of diisopropylamine (8.92 mL, 62.6 mmol) in THF (200 mL) at −78 °C under nitrogen was treated with *n*-butyllithium (1.6 M in hexanes, 36.3 mL, 58.1 mmol) dropwise, and after 5 min the mixture was warmed to 0 °C using an ice bath, stirred 30 min at this temperature, then cooled again at −78 °C. The solution was then treated with *tert*-butyl 3-oxo-8-azabicyclo[3.2.1]octane-8-carboxylate (**14**) (12.1 g, 53.6 mmol) in THF (25 mL plus 3 mL rinse), and the resulting mixture was stirred for 1 h at this temperature before being treated with 2-(4,4-difluorocyclohexyl)acetaldehyde (**13b**) (7.25 g, 44.7 mmol) in THF (25 mL plus 4 mL rinse). The resulting mixture was stirred for 2 h at this temperature then was treated with a saturated NH_4Cl aqueous solution and warmed to room temperature. The mixture was partitioned between EtOAc and water, and the layers were separated. The aqueous phase was extracted with EtOAc, and the combined organics were washed with brine, dried over $MgSO_4$, and concentrated in vacuo to give crude *tert*-butyl 2-(2-(4,4-difluorocyclohexyl)-1-hydroxyethyl)-3-oxo-8-azabicyclo[3.2.1]octane-8-carboxylate (20 g, assumed quantitative) as a pale-yellow solid which was used in the next step without further purification. Step 2: A solution of crude *tert*-butyl 2-(2-(4,4-difluorocyclohexyl)-1-hydroxyethyl)-3-oxo-8-azabicyclo[3.2.1]octane-8-carboxylate (20 g, 44.7 mmol) in CH_2Cl_2 (200 mL) at 0 °C under nitrogen was treated with NEt_3 (12.5 mL, 89.0 mmol) then methanesulfonic anhydride (8.57 g, 49.2 mmol) in CH_2Cl_2 (40 mL), and the resulting mixture was stirred at this temperature for 40 min. The organic phase was then washed with water. The aqueous phase was extracted with CH_2Cl_2, and the combined organics were washed with brine/water 1:1, dried using a phase separator, and concentrated in vacuo to give crude *tert*-butyl 2-(2-(4,4-difluorocyclohexyl)-1-((methylsulfonyl)-oxy)ethyl)-3-oxo-8-azabicyclo[3.2.1]octane-8-carboxylate (23 g, assumed quantitative) as a brown oil which was used in the next step without further purification. Step 3: A solution of crude *tert*-butyl 2-(2-(4,4-difluorocyclohexyl)-1-((methylsulfonyl)oxy)ethyl)-3-oxo-8-azabicyclo[3.2.1]octane-8-carboxylate (23 g, 44.7 mmol) in THF (100 mL) at room temperature was treated with DBU (13.5 mL, 89.0 mmol), and the resulting mixture was stirred at this temperature for 30 min then most of the solvent was removed in vacuo. The residue was partitioned between EtOAc and water and the layers were

DOI: 10.1021/acs.jmedchem.8b00862
J. Med. Chem. XXXX, XXX, XXX−XXX

separated. The aqueous phase was extracted with EtOAc and the combined organics were washed with brine, dried over $MgSO_4$, and concentrated in vacuo. Purification of the residue obtained by flash chromatography on silica gel (330 g column, 10% GLOBAL gradient (AcOEt in hexanes)) gave (*E*)-*tert*-butyl 2-(2-(4,4-difluorocyclohexyl)ethylidene)-3-oxo-8-azabicyclo[3.2.1]octane-8-carboxylate (17.94 g, 108%) as a pale-yellow oil contaminated with *tert*-butyl 3-oxo-8-azabicyclo[3.2.1]octane-8-carboxylate. This material was used in the next step without further purification. LCMS (method high pH): Retention time 1.29 min, $[M + H]^+$ = 370.4. ^1H NMR (400 MHz, $CDCl_3$) δ 6.56 (s, 1H), 5.17−4.94 (m, 1H), 4.50 (br s, 3H), 2.90−2.56 (m, 3H), 2.47−2.31 (m, 3H), 2.30−1.99 (m, 3H), 1.88−1.58 (m, 4H), 1.45 (s, 9H), 1.41−1.24 (m, 2H).

(*E*)-*tert*-Butyl-3-oxo-2-(2-(tetrahydro-2*H*-pyran-4-yl)-ethylidene)-8-azabicyclo[3.2.1]octane-8-carboxylate (15c). Step 1: A solution of diisopropylamine (6.50 mL, 45.6 mmol) in THF (150 mL) at −78 °C under nitrogen was treated with *n*-butyllithium (1.6 M in hexanes, 26.5 mL, 42.4 mmol), and after 5 min, the resulting mixture was warmed to 0 °C using an ice bath and stirred at this temperature for 30 min before being cooled again to −78 °C. The mixture was then treated with *tert*-butyl 3-oxo-8-azabicyclo[3.2.1]octane-8-carboxylate (**14**) (8.81 g, 39.1 mmol) (in 20 mL of THF) dropwise, and the mixture was stirred 90 min before being treated with crude 2-(tetrahydro-2*H*-pyran-4-yl)acetaldehyde (**13c**) (4.18 g, 32.6 mmol) in 20 mL of THF. The resulting yellow solution was stirred for 2 h at this temperature before a saturated NH_4Cl aqueous solution (100 mL) was added at −78 °C. The mixture was warmed to room temperature and diluted with EtOAc and water. The layers were separated, and the aqueous phase was extracted twice with EtOAc. The combined organics were washed with brine, dried over $MgSO_4$, and concentrated in vacuo to give 14 g of crude *tert*-butyl 2-(1-hydroxy-2-(tetrahydro-2*H*-pyran-4-yl)ethyl)-3-oxo-8-azabicyclo[3.2.1]octane-8-carboxylate as a brown oil which was used in the next step without further purification. Assumed quantitative. Step 2: A solution of crude *tert*-butyl 2-(1-hydroxy-2-(tetrahydro-2*H*-pyran-4-yl)ethyl)-3-oxo-8-azabicyclo[3.2.1]octane-8-carboxylate (14.0 g, 32,6 mmol) in CH_2Cl_2 (200 mL) at 0 °C under nitrogen was treated with NEt_3 (9.09 mL, 65.2 mmol) then with methanesulfonic anhydride (5.96 g, 34.2 mmol) in CH_2Cl_2 (20 mL). The resulting pale-yellow mixture was stirred at this temperature for 1 h then was diluted with CH_2Cl_2 and washed with water. The aqueous phase was extracted with CH_2Cl_2. The combined organics were dried using a phase separator and concentrated in vacuo to give crude *tert*-butyl 2-(1-((methylsulfonyl)oxy)-2-(tetrahydro-2*H*-pyran-4-yl)-ethyl)-3-oxo-8-azabicyclo[3.2.1]octane-8-carboxylate (15.0 g, considered quantitative) as a light-brown oil which was used in the next step without further purification. Step 3: A solution of crude *tert*-butyl 2-(1-((methylsulfonyl)oxy)-2-(tetrahydro-2*H*-pyran-4-yl)ethyl)-3-oxo-8-azabicyclo[3.2.1]octane-8-carboxylate (15.0 g, 32.6 mmol) in THF (200 mL) at room temperature was treated with DBU (9.83 mL, 65.2 mmol), and the resulting yellow-brown mixture was stirred at this temperature for 45 min then most of the THF was removed in vacuo. The residue was partitioned between EtOAc and water, and the layers were separated. The aqueous phase was extracted with EtOAc, and the combined organics were washed with brine, dried over $MgSO_4$, and concentrated in vacuo. Purification of the residue by flash chromatography on silica gel (330 G column, 40% GLOBAL gradient (AcOEt in hexanes)) gave (*E*)-*tert*-butyl 3-oxo-2-(2-(tetrahydro-2*H*-pyran-4-yl)ethylidene)-8-azabicyclo[3.2.1]octane-8-carboxylate (**15c**) (7.6 g, 70% yield over 4 steps) as a colorless oil. LCMS (method high pH): Retention time 1.09 min, $[M + H]^+$ = 336.4. ^1H NMR (400 MHz, $CDCl_3$) δ 6.63−6.51 (m, 1H), 5.18−4.96 (m, 1H), 4.58−4.40 (m, 1H), 3.97 (dt, *J* = 11.5, 2.0 Hz, 2H), 3.43−3.30 (m, 2H), 2.91−2.62 (m, 1H), 2.41 (dd, *J* = 18.1, 1.0 Hz, 1H), 2.31−2.04 (m, 4H), 1.77−1.58 (m, 5H), 1.47 (s, 9H), 1.42−1.26 (m, 2H).

(1*R,2*R**,3*S**,5*S**)-*tert*-Butyl 3-Amino-2-(2-(1,1-dioxidotetrahydro-2*H*-thiopyran-4-yl)ethyl)-8-azabicyclo[3.2.1]octane-8-carboxylate (16a).** Step 1: (*E*)-*tert*-Butyl 2-(2-(1,1-dioxidotetrahydro-2*H*-thiopyran-4-yl)ethylidene)-3-oxo-8-azabicyclo[3.2.1]-octane-8-carboxylate (**15a**) (5.5 g, 14.34 mmol) was suspended in warm MeOH (150 mL), and THF (50 mL) was added to facilitate dissolution. The suspension was then treated with palladium on carbon (10% w/w, 50% wet, 1 g), and the resulting mixture was stirred at room temperature under an atmosphere of hydrogen (1 bar) for 4 h. The catalyst was removed using a pad of Celite (2.5 g) and rinsed with AcOEt and the combined organics were concentrated in vacuo to give a white solid. Purification of this residue by flash chromatography on silica gel (25 g column, 50% Global gradient (AcOEt in hexanes)) gave (1*R**,2*S**,5*S**)-*tert*-butyl 2-(2-(1,1-dioxidotetrahydro-2*H*-thiopyran-4-yl)ethyl)-3-oxo-8-azabicyclo-[3.2.1]octane-8-carboxylate (4.1 g, 74%) as a white solid. The stereochemistry of this derivative was confirmed by NMR experiments. ^1H NMR (400 MHz DMSO-d_6): δ 4.46−4.32 (m, 1H), 4.26 (dd, *J* = 7.5, 4.0 Hz, 1H), 3.08−2.89 (m, 4H), 2.64 (dd, *J* = 15.1, 4.5 Hz, 1H), 2.49−2.43 (m, 1H), 2.20 (dd, *J* = 15.0, 1.9 Hz, 1H), 2.03 (s, 2H), 2.01−1.91 (m, 1H), 1.92−1.82 (m, 1H), 1.90−1.81 (m, 1H), 1.74−1.62 (m, 2H), 1.67−1.55 (m, 1H), 1.57−1.51 (m, 1H), 1.61−1.50 (m, 1H), 1.49 (s, 9H), 1.40−1.29 (m, 2H),1.08 (ddt, *J* = 14.0, 9.0, 7.0 Hz, 1H). Step 2: A solution of (1*R**,2*S**,5*S**)-*tert*-butyl 2-(2-(1,1-dioxidotetrahydro-2*H*-thiopyran-4-yl)ethyl)-3-oxo-8-azabicyclo-[3.2.1]octane-8-carboxylate (0.450 g, 1.17 mmol) in EtOH (20 mL) at room temperature was treated with hydroxylamine hydrochloride (0.162 g, 2.33 mmol) and pyridine (0.189 mL, 2.33 mmol), and the resulting mixture was stirred at reflux for 1 h then was cooled to room temperature and concentrated in vacuo. The residue was partitioned between CH_2Cl_2 (20 mL) and water (20 mL), and the layers were separated. The organic phase was dried using a phase separator and concentrated in vacuo to give (1*R**,2*S**,5*S**)-*tert*-butyl 2-(2-(1,1-dioxidotetrahydro-2*H*-thiopyran-4-yl)ethyl)-3-(hydroxyimino)-8-azabicyclo[3.2.1]octane-8-carboxylate (0.50 g, 107%, mixture of *Z* and *E* isomers) as a colorless oil which was used in the next step without further purification. ^1H NMR (400 MHz, $CDCl_3$) δ 7.60−7.39 (m, 1H), 4.42−4.07 (m, 2H), 3.24−3.14 (m, 1H), 3.05 (br s, 2H), 2.96 (br s, 2H), 2.61−2.33 (m, 1H), 2.11 (br s, 2H), 2.10−1.65 (m, 8H), 1.60−1.36 (m, 12H), 1.25−1.11 (m, 1H). Step 3: A solution of (1*R**,2*S**,5*S**)-*tert*-butyl 2-(2-(1,1-dioxidotetrahydro-2*H*-thiopyran-4-yl)ethyl)-3-(hydroxyimino)-8-azabicyclo[3.2.1]octane-8-carboxylate (0.30 g, 0.75 mmol) in EtOH (20 mL) at reflux under nitrogen was treated with sodium (1 g) portionwise (around 50 mg each) over 1 h, allowing effervescence to cease before adding the next piece. The mixture was then cooled to room temperature and concentrated in vacuo. The residue was partitioned between water and EtOAc, and the layers were separated. The organic phase was dried over $MgSO_4$ and concentrated in vacuo. Purification of the residue by flash chromatography on silica gel (25 g column, gradient: 0−10% (2N NH_3 in MeOH) in CH_2Cl_2) gave (1*R**,2*R**,3*S**,5*S**)-*tert*-butyl 3-amino-2-(2-(1,1-dioxidotetrahydro-2*H*-thiopyran-4-yl)ethyl)-8-azabicyclo[3.2.1]octane-8-carboxylate (**16a**) (0.22 g, 76%) as a pale-yellow gum. ^1H NMR (600 MHz, $CDCl_3$) δ 4.33−3.94 (m, 1H), 3.05 (br s, 1H), 2.97 (d, *J* = 13.6 Hz, 1H), 2.71−2.62 (m, 1H), 2.14 (br s, 2H), 2.03−1.95 (m, 1H), 1.89−1.72 (m, 7H), 1.70−1.19 (m, 19H), 1.12−1.02 (m, 1H).

(1*R,2*R**,3*S**,5*S**)-*tert*-Butyl 3-Amino-2-(2-(4,4-difluorocyclohexyl)ethyl)-8-azabicyclo[3.2.1]octane-8-carboxylate (16b).** Step 1: A solution of (*E*)-*tert*-butyl 2-(2-(4,4-difluorocyclohexyl)ethylidene)-3-oxo-8-azabicyclo[3.2.1]octane-8-carboxylate (**15b**) (14.5 g, 39.2 mmol) in MeOH (250 mL) was treated with palladium on carbon (10% w/w, 50% wet, 2 g), and the resulting mixture was stirred under an atmosphere of hydrogen for 16 h. The catalyst was filtered off using a pad of Celite (10 g) and rinsed with EtOAc and the combined organics were concentrated in vacuo. Purification of this residue by flash chromatography on silica gel (340 g column, 20% Global gradient (AcOEt in hexanes)) gave (1*R**,2*S**,5*S**)-*tert*-butyl 2-(2-(4,4-difluorocyclohexyl)ethyl)-3-oxo-8-azabicyclo[3.2.1]octane-8-carboxylate (7.07 g, 48%) as a white solid. ^1H NMR (600 MHz, DMSO-*d6*) δ 4.34−4.29 (m, 1H), 4.24−4.11 (m, 1H), 2.68−2.52 (m, 1H), 2.46−2.38 (m, 1H), 2.17 (d, *J* = 14.7 Hz, 1H), 2.03−1.93 (m, 2H), 1.96−1.89 (m, 1H), 1.91−1.80 (m, 1H), 1.85−1.78 (m, 1H), 1.80−1.69 (m, 4H), 1.53−1.45 (m, 2H), 1.44 (s, 9H), 1.38−1.29 (m, 1H), 1.26−1.20 (m, 2H),1.19−1.07 (m,

DOI: 10.1021/acs.jmedchem.8b00862
J. Med. Chem. XXXX, XXX, XXX−XXX

2H), 1.06−0.98 (m, 1H). Step 2: A solution of (1*R**,2*S**,5*S**)-*tert*-butyl 2-(2-(4,4-difluorocyclohexyl)ethyl)-3-oxo-8-azabicyclo[3.2.1]-octane-8-carboxylate (3.5 g, 9.4 mmol) in EtOH (20 mL) at room temperature was treated with hydroxylamine hydrochloride (1.31 g, 18.8 mmol) and pyridine (1.52 mL, 18.8 mmol), and the resulting mixture was stirred at reflux for 1 h then was cooled to room temperature and diluted with water (40 mL). The mixture was stirred for 30 min, then the precipitate formed was filtered off and dried under vacuum at 40 °C to give (1*R**,2*S**,5*S**)-*tert*-butyl 2-(2-(4,4-difluorocyclohexyl)ethyl)-3-(hydroxyimino)-8-azabicyclo[3.2.1]-octane-8-carboxylate (3.35 g, 92%, mixture of *Z* and *E* isomers) which was used in the next step without further purification. ^{1}H NMR (400 MHz, $CDCl_3$) δ 7.65−7.42 (m, 1H), 4.44−4.08 (m, 2H), 3.24−3.09 (m, 1H), 2.65−2.36 (m, 1H), 2.06 (br s, 4H), 1.80 (d, J = 12.5 Hz, 4H), 1.72−1.57 (m, 7H), 1.50 (s, 9H), 1.42−1.15 (m, 3H). Step 3: A solution of (1*R**,2*S**,5*S**)-*tert*-butyl 2-(2-(4,4-difluorocyclohexyl)-ethyl)-3-(hydroxyimino)-8-azabicyclo[3.2.1]octane-8-carboxylate (1.0 g, 2.6 mmol) in EtOH (60 mL) at reflux under nitrogen was treated with sodium (1 g) in small portions (around 50 mg each) over 1 h, allowing effervescence to cease before adding the next piece. The mixture was then cooled to room temperature and concentrated in vacuo. The residue was partitioned between water and EtOAc, and the layers were separated. The organic phase was dried over $MgSO_4$ and concentrated in vacuo. Purification of the residue by flash chromatography on silica gel (25 g column, gradient: 0−10% (2N NH_3 in MeOH) in CH_2Cl_2) gave (1*R**,2*R**,3*S**,5*S**)-*tert*-butyl 3-amino-2-(2-(4,4-difluorocyclohexyl)ethyl)-8-azabicyclo[3.2.1]octane-8-carboxylate (**16b**) (0.45 g, 47%) as a pale-yellow gum. ^{1}H NMR (400 MHz, DMSO-d_6) δ ppm 4.05−3.98 (m, 1H), 3.96−3.84 (m, 1H), 2.55−2.43 (m, 4H), 2.00 (d, J = 7.1 Hz, 2H), 1.89−1.58 (m, 8H), 1.56−1.23 (m, 4H), 1.45 (s, 9H), 1.16 (d, J = 10.6 Hz, 4H), 0.97−0.84 (m, 1H).

(1*R,2*R**,3*S**,5*S**)-*tert*-Butyl 3-Amino-2-(2-(tetrahydro-2*H*-pyran-4-yl)ethyl)-8-azabicyclo[3.2.1]octane-8-carboxylate (16c).** Step 1: A solution of (E)-*tert*-butyl 3-oxo-2-(2-(tetrahydro-2*H*-pyran-4-yl)ethylidene)-8-azabicyclo[3.2.1]octane-8-carboxylate (**15c**) (7.56 g, 22.5 mmol) in MeOH (150 mL) was treated with palladium on carbon (10% w/w, 50% wet, 1.5 g), and the resulting mixture was stirred under hydrogen (1 bar) at room temperature for 3 h. The catalyst was filtered off through a pad of Celite (2.5 g) and rinsed with MeOH. The combined organics were concentrated in vacuo. Purification of the residue by flash chromatography on silica gel (100 g column, 30% GLOBAL gradient (AcOEt in hexanes)) gave (1*R**,2*S**,5*S**)-*tert*-butyl 3-oxo-2-(2-(tetrahydro-2*H*-pyran-4-yl)-ethyl)-8-azabicyclo[3.2.1]octane-8-carboxylate (5.97 g, 79%) as a white foam. ^{1}H NMR (600 MHz, DMSO-d_6) δ 4.34−4.28 (m, 1H), 4.24−4.13 (m, 1H), 3.85−3.78 (m, 2H), 3.28−3.22 (m, 2H), 2.68−2.54 (m, 1H), 2.46−2.37 (m, 1H), 2.17 (d, J = 15.0 Hz, 1H), 2.00−1.89 (m, 1H), 1.87−1.75 (m, 2H), 1.56 (d, J = 12.8 Hz, 2H), 1.51−1.44 (m, 3H), 1.45 (s, 9H), 1.25−1.19 (m, 2H), 1.18−1.07 (m, 2H), 1.06−0.98 (m, 1H). Step 2: A solution of (1*R**,2*S**,5*S**)-*tert*-butyl 3-oxo-2-(2-(tetrahydro-2*H*-pyran-4-yl)ethyl)-8-azabicyclo[3.2.1]octane-8-carboxylate (0.45 g, 1.3 mmol) in EtOH (20 mL) at room temperature was treated with hydroxylamine hydrochloride (0.185 g, 2.67 mmol) and pyridine (0.216 mL, 2.67 mmol). The resulting mixture was stirred at reflux for 1 h then was cooled to room temperature and concentrated in vacuo. The residue was partitioned between CH_2Cl_2 (20 mL) and water (20 mL), and the layers were separated. The organic phase was dried using a phase separator and concentrated in vacuo to give (1*R**,2*S**,5*S**)-*tert*-butyl 3-(hydroxyimino)-2-(2-(tetrahydro-2*H*-pyran-4-yl)ethyl)-8-azabicyclo[3.2.1]-octane-8-carboxylate (0.42 g, 89%) as a colorless oil (mixture of *Z* and *E* isomers) which was used in the next step without further purification. ^{1}H NMR (400 MHz, $CDCl_3$) δ 8.97−8.69 (m, 1H), 4.44−4.09 (m, 2H), 4.02−3.84 (m, 2H), 3.37 (t, J = 11.7 Hz, 2H), 3.24−3.08 (m, 1H), 2.66−2.34 (m, 1H), 1.95 (br s, 5H), 1.61 (d, J = 13.0 Hz, 3H), 1.49 (s, 9H), 1.12−1.51 (m, 6H). Step 3: Sodium (1.0 g, 43 mmol) was cut into small pieces and placed in a beaker containing cyclohexane, then was added piece by piece over 30 min to a solution of (1*R**,2*S**,5*S**)-*tert*-butyl 3-(hydroxyimino)-2-(2-(tetrahydro-2*H*-pyran-4-yl)ethyl)-8-azabicyclo[3.2.1]octane-8-carboxylate (0.40 g, 1.1 mmol) in EtOH (30 mL) at reflux. The mixture was stirred for a further 30 min, then was cooled to room temperature and diluted with water (100 mL). The mixture was extracted with EtOAc (2 × 50 mL), and the combined organics were dried over $MgSO_4$ and concentrated in vacuo. Purification of the residue by flash chromatography on silica gel (gradient: 0−10% (2 M NH_3 in MeOH) in CH_2Cl_2) gave (1*R**,2*R**,3*S**,5*S**)-*tert*-butyl 3-amino-2-(2-(tetrahydro-2*H*-pyran-4-yl)ethyl)-8-azabicyclo[3.2.1]octane-8-carboxylate (**16**) (0.22 g, 57%) as a pale-yellow oil. ^{1}H NMR (400 MHz, $CDCl_3$) δ 4.37−4.05 (m, 2H), 3.99 (dd, J = 11.0, 3.0 Hz, 2H), 3.41 (d, J = 2.0 Hz, 2H), 2.80−2.66 (m, 1H), 2.20−1.93 (m, 3H), 1.83 (d, J = 3.3 Hz, 3H), 1.75−1.55 (m, 5H), 1.51 (s, 9H), 1.48−1.22 (m, 5H), 1.14−1.01 (m, 2H).

(3*R*,4*r*,5*S*)-*tert*-Butyl 4-Amino-3,5-dimethoxypiperidine-1-carboxylate (18a). Step 1: A solution of (3*R**,4*S**,5*S**)-*tert*-butyl 4-azido-3-hydroxy-5-methoxypiperidine-1-carboxylate (see ref 38, 560 mg, 2.06 mmol) in DMF (8 mL) at 0 °C under nitrogen was treated with sodium hydride (60% w/w in mineral oil, 99 mg, 2.5 mmol) and then after 5 min with methyl iodide (0.257 mL, 4.11 mmol). The resulting mixture was stirred for 30 min at this temperature then was diluted with water. The aqueous phase was extracted three times with Et_2O. The combined organics were washed with brine, dried over $MgSO_4$, and concentrated in vacuo. Purification of the residue by flash chromatography on silica gel (25 g column, 20% Global gradient (AcOEt in hexanes)) gave (3*R*,4*r*,5*S*)-*tert*-butyl 4-azido-3,5-dimethoxypiperidine-1-carboxylate (530 mg, 90%) as a colorless oil. ^{1}H NMR (400 MHz, $CDCl_3$) δ 4.55−4.17 (m, 2H), 3.51 (s, 6H), 3.31−3.22 (m, 1H), 3.11−2.94 (m, 2H), 2.56−2.37 (m, 2H), 1.49 (s, 9H). Step 2: A solution of (3*R*,4*r*,5*S*)-*tert*-butyl 4-azido-3,5-dimethoxypiperidine-1-carboxylate (500 mg, 1.75 mmol) in MeOH (30 mL) at room temperature was treated with palladium on carbon (10% w/w, 50% wet, 100 mg), and the resulting mixture was stirred at room temperature for 16 h under hydrogen (1 bar). The catalyst was filtered off using a pad of Celite (2.5 g) and rinsed with MeOH. The combined organics were concentrated in vacuo to give (3*R*,4*r*,5*S*)-*tert*-butyl 4-amino-3,5-dimethoxypiperidine-1-carboxylate (**18a**) (410 mg, 90%) as a black solid which was used in the next step without further purification. ^{1}H NMR (400 MHz, $CDCl_3$) δ 4.55−4.14 (m, 2H), 3.46 (s, 6H), 3.02−2.86 (m, 2H), 2.75−2.67 (m, 1H), 2.51−2.32 (m, 2H), 1.81 (br s, 2H), 1.48 (s, 9H).

(3*S,4*R**,5*R**)-*tert*-Butyl 4-amino-3-methoxy-5-((tetrahydro-2*H*-pyran-4-yl)methoxy)piperidine-1-carboxylate (18b).** Step 1: A solution of (tetrahydro-2*H*-pyran-4-yl)methanol (1.50 g, 12.9 mmol) and pyridine (1.04 mL, 12.9 mmol) in CH_2Cl_2 (30 mL) under nitrogen was cooled to 0 °C using an ice bath, then was treated with Tf_2O (2.18 mL, 12.9 mmol) dropwise. The resulting mixture was stirred for 1 h at 0 °C, then was washed with water (2 × 30 mL), dried using a phase separator, and concentrated in vacuo to give (tetrahydro-2*H*-pyran-4-yl)methyl trifluoromethanesulfonate (3.02 g, 94%) as a colorless oil which was used immediately in the next step without further purification. ^{1}H NMR (400 MHz, $CDCl_3$) δ 4.38 (d, J = 6.6 Hz, 2H), 4.08−3.98 (m, 2H), 3.42 (td, J = 11.9, 2.0 Hz, 2H), 2.19−2.06 (m, 1H), 1.74−1.64 (m, 2H), 1.50−1.35 (m, 2H). Step 2: A solution of (3*R**,4*S**,5*S**)-*tert*-butyl 4-azido-3-hydroxy-5-methoxypiperidine-1-carboxylate (0.82 g, 3.0 mmol) in THF (20 mL) under nitrogen was cooled to 0 °C using an ice bath, then was treated with potassium *tert*-butoxide (0.439 g, 3.91 mmol). The resulting mixture was stirred at this temperature for 20 min then was treated with the dropwise addition of (tetrahydro-2*H*-pyran-4-yl)methyl trifluoromethanesulfonate (1.12 g, 4.52 mmol). The resulting mixture was stirred for 1 h at 0 °C, then allowed to warm to room temperature over 1 h before being diluted with water (60 mL). The aqueous phase was extracted with EtOAc (2 × 50 mL), and the combined organics were washed with brine, dried over $MgSO_4$, and concentrated in vacuo. Purification of the residue by flash chromatography on silica gel (50 g column, gradient: 0−50% EtOAc in cyclohexane) gave (3*S**,4*R**,5*R**)-*tert*-butyl 4-azido-3-methoxy-5-((tetrahydro-2*H*-pyran-4-yl)methoxy)piperidine-1-carboxylate (0.74 g, 66%) as a pale-yellow oil. ^{1}H NMR (400 MHz, $CDCl_3$) δ 4.53−4.13 (m,

DOI: 10.1021/acs.jmedchem.8b00862
J. Med. Chem. XXXX, XXX, XXX−XXX

2H), 3.99 (dt, J = 11.5, 2.1 Hz, 2H), 3.51 (s, 3H), 3.46−3.34 (m, 3H), 3.31−3.22 (m, 1H), 3.16−3.06 (m, 1H), 2.91−3.04 (m, 1H), 2.58−2.37 (m, 2H), 1.94−1.78 (m, 1H), 1.75−1.59 (m, 3H), 1.48 (s, 9H), 1.42−1.26 (m, 2H). Step 3: A solution of (3*S**,4*R**,5*R**)-*tert*-butyl 4-azido-3-methoxy-5-((tetrahydro-2*H*-pyran-4-yl)methoxy)-piperidine-1-carboxylate (0.800 g, 2.16 mmol) in MeOH (60 mL) was hydrogenated in the H Cube over a Pd/C catalyst cartridge at atmospheric pressure. The eluant was evaporated in vacuo to give (3*S**,4*R**,5*R**)-*tert*-butyl 4-amino-3-methoxy-5-((tetrahydro-2*H*-pyran-4-yl)methoxy)piperidine-1-carboxylate (**18b**) (0.72 g, 97%) as a colorless oil, which was used in the next step without purification. ^{1}H NMR (400 MHz, $CDCl_3$) δ 4.53−4.19 (br s, 2H), 3.58−3.44 (m, 2H), 3,51 (s, 3H), 3.33−3.21 (m, 1H), 3.16−3.06 (m, 3H), 3.05−2.93 (m, 3H), 2.59−2.39 (m, 2H), 2.28−2.15 (m, 2H), 2.00−1.80 (m, 3H), 1.51−1.42 (m, 2H), 1.48 (s, 9H).

8-(((3*S*,4*R*,5*R*)-3-Methoxy-5-((tetrahydro-2*H*-pyran-4-yl)-methoxy)piperidin-4-yl)amino)-3-methyl-5-(5-methylpyridin-3-yl)-1,7-naphthyridin-2(1*H*)-one (22). Step 1: A mixture of (3*S**,4*R**,5*R**)-*tert*-butyl 4-amino-3-methoxy-5-((tetrahydro-2*H*-pyran-4-yl)methoxy)piperidine-1-carboxylate (**18b**) (0.200 g, 0.579 mmol), 2-(benzyloxy)-8-chloro-3-methyl-1,7-naphthyridine (**19a**) (0.15 g, 0.53 mmol), sodium *tert*-butoxide (0.152 g, 1.58 mmol), BrettPhos (0.028 g, 0.053 mmol), and $Pd_2(dba)_3$ (0.024 g, 0.026 mmol) in THF (2 mL) was stirred at room temperature for 1 h, then at 60 °C for 18 h before being cooled to room temperature and diluted with EtOAc (20 mL). The organic phase was washed with water, dried over $MgSO_4$, and concentrated in vacuo. Purification of the residue by flash chromatography on silica gel (25 g column, gradient: 0−100% EtOAc in cyclohexane) gave (3*S**,4*R**,5*R**)-*tert*-butyl 4-((2-(benzyloxy)-3-methyl-1,7-naphthyridin-8-yl)amino)-3-methoxy-5-((tetrahydro-2*H*-pyran-4-yl)methoxy)piperidine-1-carboxylate (0.12 g, 38%) as a pale-yellow gum. LCMS (method high pH): Retention time 1.42 min, $[M + H]^+$ = 593. ^{1}H NMR (400 MHz, $CDCl_3$) δ 7.92 (d, J = 5.9 Hz, 1H), 7.68 (s, 1H), 7.55−7.47 (m, 2H), 7.45−7.38 (m, 2H), 7.35 (d, J = 7.1 Hz, 1H), 6.73 (d, J = 5.6 Hz, 1H), 6.25 (d, J = 9.0 Hz, 1H), 5.52 (s, 2H), 4.58−4.24 (m, 2H), 3.69−3.31 (m, 9H), 3.08−2.86 (m, 3H), 2.83−2.63 (m, 2H), 2.41 (s, 3H), 1.54 (s, 9H), 1.45−1.34 (m, 1H), 1.29−1.16 (m, 1H), 1.14−1.03 (m, 1H), 1.01−0.87 (m, 1H), 0.80−0.64 (m, 1H). Step 2: A solution of (3*S**,4*R**,5*R**)-*tert*-butyl 4-((2-(benzyloxy)-3-methyl-1,7-naphthyridin-8-yl)amino)-3-methoxy-5-((tetrahydro-2*H*-pyran-4-yl)-methoxy)piperidine-1-carboxylate (130 mg, 0.219 mmol) in CH_2Cl_2 (10 mL) was cooled using an ice bath then was treated with NBS (39.0 mg, 0.219 mmol), and the resulting mixture was stirred at this temperature for 1 h. The mixture was then treated with a saturated aqueous sodium metabisulphite solution, and after 10 min the layers were separated. The organic phase was dried using a phase separator and concentrated in vacuo to give (3*S**,4*R**,5*R**)-*tert*-butyl 4-((2-(benzyloxy)-5-bromo-3-methyl-1,7-naphthyridin-8-yl)amino)-3-methoxy-5-((tetrahydro-2*H*-pyran-4-yl)methoxy)piperidine-1-carboxylate (0.15 g, 102%) which was used in the next step without further purification.

LCMS (method high pH): Retention time 1.56 min, $[M + H]^+$ = 673.6 (1 Br). ^{1}H NMR (400 MHz, $CDCl_3$) δ ppm 8.05 (s, 1H), 7.99 (d, J = 1.0 Hz, 1H), 7.50 (d, J = 6.8 Hz, 2H), 7.39−7.44 (m, 2H), 7.33−7.38 (m, 1H), 6.26 (d, J = 9.3 Hz, 1H), 5.52 (s, 2H), 4.17−4.57 (m, 2H), 4.05−4.16 (m, 1H), 3.59−3.73 (m, 2H), 3.43−3.59 (m, 2H), 3.38 (s, 3H), 3.32−3.37 (m, 1H), 2.94−3.11 (m, 3H), 2.60−2.78 (m, 2H), 2.47 (d, J = 1.0 Hz, 3H), 1.54 (s, 9H), 1.39−1.50 (m, 1H), 1.21−1.30 (m, 1H), 1.08−1.17 (m, 1H), 0.98 (qd, J = 12.3, 4.6 Hz, 1H), 0.68−0.82 (m, 1H). Step 3: A 20 mL microwave vial was charged with (5-methylpyridin-3-yl)boronic acid (0.046 g, 0.335 mmol), (3*S**,4*R**,5*R**)-*tert*-butyl 4-((2-(benzyloxy)-5-bromo-3-methyl-1,7-naphthyridin-8-yl)amino)-3-methoxy-5-((tetrahydro-2*H*-pyran-4-yl)methoxy)piperidine-1-carboxylate (0.150 g, 0.223 mmol), K_2CO_3 (0.093 g, 0.67 mmol), $Pd(OAc)_2$ (5.0 mg, 0.022 mmol), di((3*S*,5*S*,7*S*)-adamantan-1-yl)(butyl)phosphine (cataCXium A) (8.0 mg, 0.022 mmol), and then was filled with 1,4-dioxane (4 mL), and water (2 mL). The reaction mixture was stirred and degassed for 20 min with nitrogen. The reaction vessel was sealed and the mixture was stirred under microwave irradiations at 100 °C for 30 min then was cooled to room temperature and concentrated in vacuo. The residue was partitioned between CH_2Cl_2 (20 mL) and water (20 mL), and the layers were separated. The organic phase was dried through a hydrophobic frit and concentrated in vacuo to give a brown residue. This was dissolved in TFA (2 mL), reluxed for 4 h, then cooled to room temperature and concentrated in vacuo. Purification of the residue by MDAP (method high pH) gave 8-(((3*S**,4*R**,5*R**)-3-methoxy-5-((tetrahydro-2*H*-pyran-4-yl)methoxy)piperidin-4-yl)-amino)-3-methyl-5-(5-methylpyridin-3-yl)-1,7-naphthyridin-2(1*H*)-one (58 mg, 53%) as a white foam. LCMS (method high pH): Retention time 0.69 min, $[M + H]^+$ = 494.5. ^{1}H NMR (400 MHz, $CDCl_3$) δ ppm 12.93−13.92 (m, 1H), 8.52 (d, J = 1.5 Hz, 1H), 8.47 (d, J = 2.0 Hz, 1H), 7.96 (s, 1H), 7.75 (d, J = 1.0 Hz, 1H), 7.52 (d, J = 1.0 Hz, 1H), 6.60−6.81 (m, 1H), 4.54−4.73 (m, 1H), 3.77 (br dd, J = 11.2, 2.4 Hz, 1H), 3.48 (br d, J = 3.9 Hz, 3H), 3.45 (s, 4H), 3.34−3.40 (m, 1H), 3.33−3.42 (m, 1H), 3.25 (dd, J = 8.8, 7.3 Hz, 1H), 3.17−3.22 (m, 1H), 3.11−3.16 (m, 1H), 2.59−2.69 (m, 2H), 2.46 (s, 3H), 2.36 (d, J = 1.0 Hz, 3H), 1.67 (br s, 3H), 1.37 (br dd, J = 13.0, 1.7 Hz, 1H), 1.24−1.32 (m, 1H), 1.11 (qd, J = 12.4, 4.4 Hz, 1H). The two enantiomers of 8-(((3*S**,4*R**,5*R**)-3-methoxy-5-((tetrahydro-2*H*-pyran-4-yl)methoxy)piperidin-4-yl)amino)-3-methyl-5-(5-methylpyridin-3-yl)-1,7-naphthyridin-2(1*H*)-one were separated by chiral chromatograhy. Analytical method: Approximately 0.5 mg of racemate were dissolved in 50% EtOH in heptane (1 mL) and 20 μL were injected onto the column, eluting with 30% EtOH (+0.2% isopropylamine) in heptane, f = 1.0 mL/min, wavelength 215 nm. Column 4.6 mm i.d. × 25 cm Chiralcel OD-H. Preparative method: approximately 44 mg of material were dissolved in 3 mL of EtOH (+0.2% isopropylamine). Injections (3 in total): 1 mL of the solution was injected onto the column eluting with 30% EtOH (+0.2% isopropylamine) in heptane, f = 25 mL/min, wavelength 215 nm. Column 30 mm × 25 cm Chiralcel OD-H. The appropriate fractions were combined and concentrated in vacuo to give 8-(((3*S*,4*R*,5*R*)-3-methoxy-5-((tetrahydro-2*H*-pyran-4-yl)methoxy)piperidin-4-yl)-amino)-3-methyl-5-(5-methylpyridin-3-yl)-1,7-naphthyridin-2(1*H*)-one (13 mg, 59%) as the fastest running enantiomer and 8-(((3*R*,4*S*,5*S*)-3-methoxy-5-((tetrahydro-2*H*-pyran-4-yl)methoxy)-piperidin-4-yl)amino)-3-methyl-5-(5-methylpyridin-3-yl)-1,7-naphthyridin-2(1*H*)-one (11 mg, 50%) as the slowest running enantiomer.

3-Methyl-5-(5-methylpyridin-3-yl)-8-(((1*S*,2*R*,3*R*,5*R*)-2-(2-(tetrahydro-2*H*-pyran-4-yl)ethyl)-8-azabicyclo[3.2.1]octan-3-yl)amino)-1,7-naphthyridin-2(1*H*)-one (23). Step 1: A mixture of (1*R**,2*R**,3*S**,5*S**)-*tert*-butyl 3-amino-2-(2-(tetrahydro-2*H*-pyran-4-yl)ethyl)-8-azabicyclo[3.2.1]octane-8-carboxylate (**16c**) (0.18 g, 0.53 mmol), 2-(benzyloxy)-8-chloro-3-methyl-1,7-naphthyridine (**19a**) (0.15 g, 0.53 mmol), sodium *tert*-butoxide (0.152 g, 1.58 mmol), BrettPhos (0.028 g, 0.053 mmol), and $Pd_2(dba)_3$ (0.024 g, 0.026 mmol) in THF (2 mL) was stirred at room temperature for 1 h, then at 60 °C for 18 h. The mixture was then cooled to room temperature and diluted with EtOAc (20 mL). The organic phases was washed with water, dried over $MgSO_4$, and concentrated in vacuo. Purification of the residue by flash chromatography on silica gel (25 g column, gradient 0−80% EtOAc in cyclohexane) gave (1*S**,2*S**,3*R**,5*R**)-*tert*-butyl 3-((2-(benzyloxy)-3-methyl-1,7-naphthyridin-8-yl)amino)-2-(2-(tetrahydro-2*H*-pyran-4-yl)ethyl)-8-azabicyclo[3.2.1]octane-8-carboxylate (0.245 g, 79%). LCMS (method high pH): Retention time 1.08 min, $[M + H]^+$ = 587.6. ^{1}H NMR (400 MHz, $CDCl_3$) δ 7.86 (d, J = 5.6 Hz, 1H), 7.65 (d, J = 1.0 Hz, 1H), 7.52−7.46 (m, 2H), 7.45−7.39 (m, 2H), 7.37−7.30 (m, 1H), 6.70 (d, J = 5.9 Hz, 1H), 5.92 (d, J = 9.0 Hz, 1H), 5.49 (s, 2H), 4.30 (br s, 3H), 3.87 (dd, J = 11.0, 2.7 Hz, 2H), 3.34−3.21 (m, 2H), 2.79 (s, 1H), 2.45 (d, J = 1.0 Hz, 3H), 2.15−1.99 (m, 2H), 1.99−1.80 (m, 3H), 1.79−1.43 (m, 14H), 1.37 (d, J = 10.5 Hz, 2H), 1.29−1.08 (m, 3H). Step 2: A solution of (1*S**,2*S**,3*R**,5*R**)-*tert*-butyl 3-((2-(benzyloxy)-3-methyl-1,7-naphthyridin-8-yl)amino)-2-(2-(tetrahydro-2*H*-pyran-4-yl)ethyl)-8-azabicyclo[3.2.1]octane-8-carboxylate (0.18 g, 0.31 mmol) in CH_2Cl_2 (10 mL) at 0 °C was treated with NBS (0.055 g, 0.31 mmol), and the resulting mixture was stirred at this temperature for 1 h then was treated with a 10% w/w sodium metabisulphite aqueous solution. The

DOI: 10.1021/acs.jmedchem.8b00862
J. Med. Chem. XXXX, XXX, XXX−XXX

biphasic mixture was stirred for 20 min, and then the layers were separated. The organic layer was dried using an hydrophobic frit and concentrated in vacuo to give (1*S**,2*S**,3*R**,5*R**)-*tert*-butyl 3-((2-(benzyloxy)-5-bromo-3-methyl-1,7-naphthyridin-8-yl)amino)-2-(2-(tetrahydro-2*H*-pyran-4-yl)ethyl)-8-azabicyclo[3.2.1]octane-8-carboxylate (0.21 g, 103%) as an orange foam which was used in the next step without further purification. LCMS (method high pH): Retention time 1.71 min, $[M + H]^+$ = 667.5 (1 Br). ^{1}H NMR (400 MHz, $CDCl_3$) δ 7.98 (s, 1H), 7.96 (d, J = 1.2 Hz, 1H), 7.50-.46 (m, 2H) 7.45−7.39 (m, 2H), 7.38−7.32 (m, 1H), 5.92 (d, J = 9.0 Hz, 1H), 5.49 (s, 2H), 4.30 (br s, 3H), 3.87 (dd, J = 11.0, 2.7 Hz, 2H), 3.34−3.21 (m, 2H), 2.45 (d, J = 1.0 Hz, 3H), 2.15−1.99 (m, 2H), 1.99−1.79 (m, 3H), 1.78−1.30 (m, 8H), 1.55 (s, 9H), 1.29−1.08 (m, 3H). Step 3: A 20 mL microwave vial was charged with (5-methylpyridin-3-yl)boronic acid (0.062 g, 0.45 mmol), (1*S**,2*S**,3*R**,5*R**)-*tert*-butyl 3-((2-(benzyloxy)-5-bromo-3-methyl-1,7-naphthyridin-8-yl)amino)-2-(2-(tetrahydro-2*H*-pyran-4-yl)ethyl)-8-azabicyclo[3.2.1]octane-8-carboxylate (0.20 g, 0.30 mmol), K_2CO_3 (0.125 g, 0.901 mmol), $Pd(OAc)_2$ (6.75 mg, 0.030 mmol), cataCXium A (10.8 mg, 0.0300 mmol), then was filled with 1,4-dioxane (4 mL) and water (2 mL). The resulting mixture was stirred and degassed for 20 min with nitrogen. The mixture was then stirred at 100 °C for 30 min under microwave irradiations then was cooled to room temperature and concentrated in vacuo. The residue was partitioned between CH_2Cl_2 (20 mL) and water (20 mL), and the layers were separated. The organic layer was dried using an hydrophobic frit and concentrated in vacuo. Purification of the residue by flash chromatography on silica gel (25 g column, gradient 0−100% EtOAc in cyclohexane) gave (1*S**,2*S**,3*R**,5*R**)-*tert*-butyl 3-((2-(benzyloxy)-3-methyl-5-(5-methylpyridin-3-yl)-1,7-naphthyridin-8-yl)amino)-2-(2-(tetrahydro-2*H*-pyran-4-yl)ethyl)-8-azabicyclo-[3.2.1]octane-8-carboxylate (145 mg, 71%) as a pale-yellow gum. This product was dissolved in TFA (2 mL), and the resulting solution was stirred at reflux for 3 h then was cooled to room temperature and concentrated in vacuo. The residue was dissolved in MeOH and loaded onto a 5 g SCX2 cartridge, which was washed with MeOH (10 mL) then eluted with a 2N NH_3 solution in MeOH. The eluant was evaporated in vacuo to give 3-methyl-5-(5-methylpyridin-3-yl)-8-(((1*S**,2*R**,3*R**,5*R**)-2-(2-(tetrahydro-2*H*-pyran-4-yl)ethyl)-8-azabicyclo[3.2.1]octan-3-yl)amino)-1,7-naphthyridin-2(1*H*)-one (92 mg, 63%) as a pale-yellow foam. LCMS (method high pH): Retention time 0.82 min, $[M + H]^+$ = 488.6. ^{1}H NMR (400 MHz, DMSO-d_6) δ 8.44 (d, J = 1.5 Hz, 1H), 8.37 (d, J = 1.8 Hz, 1H), 7.70 (s, 1H), 7.59−7.56 (m, 1H), 7.48 (d, J = 1.3 Hz, 1H), 6.55 (d, J = 8.1 Hz, 1H), 4.27 (br s, 1H), 3.80−3.71 (m, 2H), 3.64−3.57 (m, 1H), 3.53 (d, J = 3.8 Hz, 1H), 3.28−3.19 (m, 2H), 2.85 (br s 2H), 2.40 (s, 3H), 2.11 (d, J = 1.3 Hz, 3H), 2.04−1.96 (m, 1H), 1.91−1.65 (m, 6H), 1.64−1.44 (m, 4H), 1.44−1.28 (m, 2H), 1.28−1.17 (m, 1H), 1.16−1.00 (m, 2H). Step 4: The two enantiomers of 3-methyl-5-(5-methylpyridin-3-yl)-8-(((1*S**,2*R**,3*R**,5*R**)-2-(2-(tetrahydro-2*H*-pyran-4-yl)ethyl)-8-azabicyclo[3.2.1]octan-3-yl)amino)-1,7-naphthyridin-2(1*H*)-one were separated by chiral chromatography. Analytical method: approximately 0.5 mg of racemate were dissolved in 1:1 EtOH/heptane (1 mL). Then 20 μL were injected on column. Eluant: 50% EtOH (+0.2% isopropylamine) in heptane, f = 1.0 mL/min, wavelength 215 nm. Column 4.6 mm i.d. × 25 cm Chiralpak IC. Preparative method: 35 mg of racemate were dissolved in EtOH (1 mL) then were injected onto the column. Eluant: 40% EtOH (+0.2% isopropylamine) in heptane, f = 15 mL/min, wavelength = 215 nm. Column 2 cm × 25 cm Chiralpak IC. Total number of injection: 1. The fractions were collected to give 3-methyl-5-(5-methylpyridin-3-yl)-8-(((1*S*,2*R*,3*R*,5*R*)-2-(2-(tetrahydro-2*H*-pyran-4-yl)ethyl)-8-azabicyclo[3.2.1]octan-3-yl)amino)-1,7-naphthyridin-2(1*H*)-one (**22**) (13 mg, 74%) as the fastest running enantiomer and 3-methyl-5-(5-methylpyridin-3-yl)-8-(((1*R*,2*S*,3*S*,5*S*)-2-(2-(tetrahydro-2*H*-pyran-4-yl)ethyl)-8-azabicyclo[3.2.1]octan-3-yl)amino)-1,7-naphthyridin-2(1*H*)-one (11 mg, 63%) as slowest running enantiomer.

8-(((1*S*,2*R*,3*R*,5*R*)-2-(2-(1,1-Dioxidotetrahydro-2*H*-thiopyran-4-yl)ethyl)-8-azabicyclo[3.2.1]octan-3-yl)amino)-3-methyl-5-(5-methylpyridin-3-yl)-1,7-naphthyridin-2(1*H*)-one (24). Step 1: A mixture of (1*R**,2*R**,3*S**,5*S**)-*tert*-butyl 3-amino-2-(2-(1,1-dioxidotetrahydro-2*H*-thiopyran-4-yl)ethyl)-8-azabicyclo[3.2.1]-octane-8-carboxylate (**16a**) (0.22 g, 0.57 mmol), 2-(benzyloxy)-8-chloro-3-methyl-1,7-naphthyridine (**19a**) (0.15 g, 0.53 mmol), sodium *tert*-butoxide (0.152 g, 1.58 mmol), BrettPhos (0.028 g, 0.053 mmol), and $Pd_2(dba)_3$ (0.024 g, 0.026 mmol) in THF (2 mL) was stirred at room temperature for 1 h then at 60 °C for 18 h. The mixture was cooled to room temperature and diluted with EtOAc (20 mL). The organic phase was washed with water, dried over $MgSO_4$, and concentrated in vacuo. Purification of the residue by flash chromatography on silica gel (25 g column, gradient: 0−80% EtOAc in cyclohexane) gave (1*S**,2*S**,3*R**,5*R**)-*tert*-butyl 3-((2-(benzyloxy)-3-methyl-1,7-naphthyridin-8-yl)amino)-2-(2-(1,1-dioxidotetrahydro-2*H*-thiopyran-4-yl)ethyl)-8-azabicyclo[3.2.1]octane-8-carboxylate (135 mg, 40%) as a pale-yellow foam. LCMS (method TFA): Retention time 1.06 min, $[M + H]^+$ = 635. ^{1}H NMR (600 MHz, $CDCl_3$) δ 7.84 (d, J = 5.6 Hz, 1H), 7.66 (d, J = 1.0 Hz, 1H), 7.51−7.46 (m, 2H), 7.45−7.38 (m, 2H), 7.35 (d, J = 7.3 Hz, 1H), 6.70 (d, J = 5.9 Hz, 1H), 5.90 (d, J = 9.8 Hz, 1H), 5.54−5.42 (m, 2H), 4.46−4.18 (m, 3H), 2.94−2.70 (m, 4H), 2.40 (d, J = 1.0 Hz, 3H), 2.06 (s, 6H), 1.98−1.80 (m, 6H), 1.79−1.57 (m, 2H), 1.54 (s, 9H), 1.27 (m, J = 7.2 Hz, 2H). Step 2: A solution of (1*S**,2*S**,3*R**,5*R**)-*tert*-butyl 3-((2-(benzyloxy)-3-methyl-1,7-naphthyridin-8-yl)amino)-2-(2-(1,1-dioxidotetrahydro-2*H*-thiopyran-4-yl)ethyl)-8-azabicyclo[3.2.1]octane-8-carboxylate (0.13 g, 0.21 mmol) in CH_2Cl_2 (10 mL) was cooled using an ice bath then was treated with NBS (0.036 g, 0.205 mmol) in two portions, of 22 mg and 14 mg, with 2 min stirring interval between additions. The mixture was then treated with a 10% w/w sodium metabisulphite aqueous solution, and the layers were separated. The organic phase was dried using a phase separator and concentrated in vacuo to give (1*S**,2*S**,3*R**,5*R**)-*tert*-butyl 3-((2-(benzyloxy)-5-bromo-3-methyl-1,7-naphthyridin-8-yl)amino)-2-(2-(1,1-dioxidotetrahydro-2*H*-thiopyran-4-yl)ethyl)-8-azabicyclo[3.2.1]-octane-8-carboxylate (0.15 g, 103%) as an orange foam which was used in the next step without further purification. LCMS (method high pH): Retention time 1.62 min. $[M + H]^+$ = 715.5 (1 Br). ^{1}H NMR (400 MHz, $CDCl_3$) δ 8.01−7.94 (m, 1H), 7.50−7.40 (m, 2H), 7.36 (d, J = 7.1 Hz, 1H), 5.89 (d, J = 9.5 Hz, 1H), 5.49 (d, J = 5.1 Hz, 2H), 4.45−4.08 (m, 3H), 3.02−2.80 (m, 4H), 2.46 (d, J = 1.0 Hz, 3H), 2.13−1.80 (m, 8H), 1.79−1.61 (m, 5H), 1.57−1.52 (m, 10H), 1.45 (s, 5H). Step 3: A 20 mL microwave vial was charged with (5-methylpyridin-3-yl)boronic acid (0.043 g, 0.32 mmol), (1*S**,2*S**,3*R**,5*R**)-*tert*-butyl 3-((2-(benzyloxy)-5-bromo-3-methyl-1,7-naphthyridin-8-yl)amino)-2-(2-(1,1-dioxidotetrahydro-2*H*-thiopyran-4-yl)ethyl)-8-azabicyclo[3.2.1]octane-8-carboxylate (0.15 g, 0.21 mmol), K_2CO_3 (0.087 g, 0.63 mmol), $Pd(OAc)_2$ (4.7 mg, 0.021 mmol), and di((3*S*,5*S*,7*S*)-adamantan-1-yl)(butyl)phosphine (cataCXium A) (7.5 mg, 0.021 mmol) then was filled with 1,4-dioxane (4 mL), and water (2 mL). The resulting mixture was stirred and degassed for 20 min with nitrogen then was stirred at 100 °C for 30 min under microwave irradiations before being cooled to room temperature and concentrated in vacuo. The residue was partitioned between CH_2Cl_2 (20 mL) and water (20 mL), and the layers were separated. The organic phase was dried using an hydrophobic frit and concentrated in vacuo. Purification of the residue by flash chromatography on silica gel (25 g column, gradient: 0−100% EtOAc in cyclohexane) gave (1*S**,2*S**,3*R**,5*R**)-*tert*-butyl 3-((2-(benzyloxy)-3-methyl-5-(5-methylpyridin-3-yl)-1,7-naphthyridin-8-yl)amino)-2-(2-(1,1-dioxidotetrahydro-2*H*-thiopyran-4-yl)ethyl)-8-azabicyclo[3.2.1]octane-8-carboxylate (0.122 g, 80%) as a yellow gum. LCMS (method high pH): Retention time 1.46 min, $[M + H]^+$ = 726. ^{1}H NMR (400 MHz, $CDCl_3$) δ 8.51−8.47 (m, 1H), 7.80 (s, 1H), 7.74−7.68 (m, 1H), 7.56−7. 47 (m, 3H), 7.46−7.40 (m, 3H), 7.36 (d, J = 7.3 Hz, 1H), 6.02 (d, J = 9.8 Hz, 1H), 5.56−5.46 (m, 2H), 4.52−4.38 (m, 2H), 4.37−4.12 (m, 2H), 2.99−2.74 (m, 6H), 2.44 (s, 3H), 2.37 (d, J = 1.0 Hz, 3H), 2.15−1.82 (m, 8H), 1.80−1.60 (m, 5H), 1.56 (s, 6H), 1.49−1.15 (m, 3H). Step 4: A solution of (1*S**,2*S**,3*R**,5*R**)-*tert*-butyl 3-((2-(benzyloxy)-3-methyl-5-(5-methylpyridin-3-yl)-1,7-naphthyridin-8-yl)amino)-2-(2-(1,1-dioxidotetrahydro-2*H*-thiopyran-4-yl)ethyl)-8-azabicyclo[3.2.1]octane-8-carboxy-

DOI: 10.1021/acs.jmedchem.8b00862
J. Med. Chem. XXXX, XXX, XXX−XXX

late (0.12 g, 0.16 mmol) in TFA (1 mL) was refluxed for 4 h then was allowed to stand at room temperature for 48 h before being concentrated in vacuo. The brown residue obtained was purified by MDAP (method high pH). The residue obtained was further purified by MDAP (method formic) to give 8-(((1*S**,2*R**,3*R**,5*R**)-2-(2-(1,1-dioxidotetrahydro-2*H*-thiopyran-4-yl)ethyl)-8-azabicyclo[3.2.1]-octan-3-yl)amino)-3-methyl-5-(5-methylpyridin-3-yl)-1,7-naphthyridin-2(1*H*)-one (60 mg, 68%) as a pale-yellow solid. LCMS (method high pH): Retention time 0.74 min, $[M + H]^+$ = 536. ^{1}H NMR (400 MHz, $CDCl_3$) δ 8.52 (br s, 1H), 8.46 (br s, 1H), 7.85−7.79 (m, 1H), 7.78 (s, 1H), 7.59 (d, *J* = 3.7 Hz, 2H), 4.61−4.45 (m, 1H), 4.18 (d, *J* = 4.9 Hz, 1H), 4.11 (br s, 1H), 3.12−2.88 (m, 4H), 2.48 (s, 3H), 2.33 (d, *J* = 12.0 Hz, 3H), 2.19 (s, 6H), 2.04 (d, *J* = 11.0 Hz, 3H), 1.78 (br s, 4H), 1.40 (br s, 2H), 1.34−1.19 (m, 1H). Step 5: The two enantiomers of 8-(((1*S**,2*R**,3*R**,5*R**)-2-(2-(1,1-dioxidotetrahydro-2*H*-thiopyran-4-yl)ethyl)-8-azabicyclo[3.2.1]octan-3-yl)amino)-3-methyl-5-(5-methylpyridin-3-yl)-1,7-naphthyridin-2(1*H*)-one were separated by chiral chromatography. Analytical method: Approximately 0.5 mg of material were dissolved in 50% EtOH in heptane (1 mL) and 20 μL were injected onto the column. Eluant: 70% EtOH (+0.2% isopropylamine) in heptane, *f* = 1.0 mL/min, wavelength = 215 nm. Column 4.6 mm i.d. × 25 m Chiralpak IC. Preparative method: Approximately 50 mg of material were dissolved in EtOH (1 mL) and isopropylamine (100 μL). The solution was injected onto the column. Eluant: 70% EtOH (+0.2% isopropylamine) in heptane, *f* = 25 mL/min, wavelength 215 nm. Column 30 mm × 25 cm Chiralpak IC. The appropriate fractions were collected and concentrated in vacuo to give 8-(((1*S*,2*R*,3*R*,5*R*)-2-(2-(1,1-dioxidotetrahydro-2*H*-thiopyran-4-yl)ethyl)-8-azabicyclo[3.2.1]octan-3-yl)-amino)-3-methyl-5-(5-methylpyridin-3-yl)-1,7-naphthyridin-2(1*H*)-one (**24**) (13 mg, 52%) as the fastest running enantiomer and 8-(((1*R*,2*S*,3*S*,5*S*)-2-(2-(1,1-dioxidotetrahydro-2*H*-thiopyran-4-yl)-ethyl)-8-azabicyclo[3.2.1]octan-3-yl)amino)-3-methyl-5-(5-methyl-pyridin-3-yl)-1,7-naphthyridin-2(1*H*)-one (13 mg, 52%) as the slowest running enantiomer. Each product was obtained as pale-yellow solid.

8-(((1*S*,2*S*,3*S*,5*R*)-2-(2-(4,4-Difluorocyclohexyl)ethyl)-8-azabicyclo[3.2.1]octan-3-yl)amino)-3-methyl-5-(5-methylpyridin-3-yl)-1,7-naphthyridin-2(1*H*)-one (26). Step 1: A mixture of (1*R**,2*R**,3*S**,5*S**)-*tert*-butyl 3-amino-2-(2-(4,4-difluorocyclohexyl)-ethyl)-8-azabicyclo[3.2.1]octane-8-carboxylate (**16b**), (0.36 g, 0.97 mmol), 2-(benzyloxy)-8-chloro-3-methyl-1,7-naphthyridine (**19a**) (0.25 g, 0.88 mmol), sodium *tert*-butoxide (0.253 g, 2.63 mmol), BrettPhos (0.094 g, 0.18 mmol), and $Pd_2(dba)_3$ (0.080 g, 0.088 mmol) in THF (2 mL) was stirred at room temperature for 1 h then at 60 °C for 18 h. The mixture was then cooled to room temperature and diluted with EtOAc (20 mL). The mixture was washed with water, dried over $MgSO_4$, and concentrated in vacuo. Purification of the residue by flash chromatography on silica gel (25 g column, gradient: 0−80% EtOAc in cyclohexane) gave (1*S**,2*S**,3*R**,5*R**)-*tert*-butyl 3-((2-(benzyloxy)-3-methyl-1,7-naphthyridin-8-yl)amino)-2-(2-(4,4-difluorocyclohexyl)ethyl)-8-azabicyclo[3.2.1]octane-8-carboxylate (0.51 g, 94%). LCMS (method high pH): Retention time 1.27 min, $[M + H]^+$ = 621. ^{1}H NMR (400 MHz, $CDCl_3$) δ 7.86 (d, *J* = 5.6 Hz, 1H), 7.65 (d, *J* = 1.0 Hz, 1H), 7.52−7.46 (m, 2H), 7.46−7.39 (m, 2H), 7.35 (d, *J* = 7.3 Hz, 1H), 6.70 (d, *J* = 5.6 Hz, 1H), 5.92 (d, *J* = 9.3 Hz, 1H), 5.49 (d, *J* = 2.9 Hz, 2H), 4.45−4.12 (m, 3H), 2.40 (d, *J* = 1.0 Hz, 3H), 2.20−1.83 (m, 8H), 1.80−1.58 (m, 7H), 1.55 (s, 9H), 1.42−1.06 (m, 5H). Step 2: A solution of (1*S**,2*S**,3*R**,5*R**)-*tert*-butyl 3-((2-(benzyloxy)-3-methyl-1,7-naphthyridin-8-yl)amino)-2-(2-(4,4-difluorocyclohexyl)ethyl)-8-azabicyclo[3.2.1]octane-8-carboxylate (0.30 g, 0.48 mmol) in CH_2Cl_2 (10 mL) was cooled using an ice bath then was treated with the portionwise addition of NBS (0.086 g, 0.48 mmol) with a 10 min stirring interval between additions. The resulting mixture was stirred for 20 min then was treated with a 10% w/w sodium metabisulphite aqueous solution. The layers were separated, and the organic phase was dried over $MgSO_4$ and concentrated in vacuo to give (1*S**,2*S**,3*R**,5*R**)-*tert*-butyl 3-((2-(benzyloxy)-5-bromo-3-methyl-1,7-naphthyridin-8-yl)amino)-2-(2-(4,4-difluorocyclohexyl)ethyl)-8-azabicyclo[3.2.1]octane-8-carboxylate (0.35 g, 104%) as a pale-yellow foam which was used in the next step without further purification. LCMS (method high pH): Retention time 1.84 min, $[M + H]^+$ = 699/701 (1 Br). ^{1}H NMR (400 MHz, $CDCl_3$) δ 7.98 (s, 1H), 7.96 (d, *J* = 1.0 Hz, 1H), 7.50−7.46 (m, 2H), 7.45−7.39 (m, 2H), 7.35 (d, *J* = 7.1 Hz, 1H), 5.91 (d, *J* = 9.5 Hz, 1H), 5.49 (d, *J* = 2.4 Hz, 2H), 4.31 (m, 3H), 2.45 (d, *J* = 1.0 Hz, 3H), 2.13−1.79 (m, 8H), 1.75−1.46 (m, 14H), 1.43- 1.06 (m, 7H). Step 3: A 20 mL microwave vial was charged with (5-methylpyridin-3-yl)boronic acid (0.103 g, 0.750 mmol), (1*S**,2*S**,3*R**,5*R**)-*tert*-butyl 3-((2-(benzyloxy)-5-bromo-3-methyl-1,7-naphthyridin-8-yl)amino)-2-(2-(4,4-difluorocyclohexyl)-ethyl)-8-azabicyclo[3.2.1]octane-8-carboxylate (0.35 g, 0.50 mmol), K_2CO_3 (0.207 g, 1.50 mmol), $Pd(OAc)_2$ (0.011 g, 0.050 mmol), and di((3*S*,5*S*,7*S*)-adamantan-1-yl)(butyl)phosphine (cataCXium A) (0.018 g, 0.050 mmol) then was filled with 1,4-dioxane (4 mL), and water (2 mL). The resulting mixture was stirred and degassed for 20 min with nitrogen, was stirred at 100 °C for 30 min under microwave irradiations, and then was cooled to room temperature and concentrated in vacuo. The residue was partitioned between CH_2Cl_2 (20 mL) and water (20 mL), and the layers were separated. The organic phase was dried using an hydrophobic frit and concentrated in vacuo. Purification of the residue by flash chromatography on silica gel (25 g column, gradient: 0−100% EtOAc in cyclohexane) gave (1*S**,2*S**,3*R**,5*R**)-*tert*-butyl 3-((2-(benzyloxy)-3-methyl-5-(5-methylpyridin-3-yl)-1,7-naphthyridin-8-yl)amino)-2-(2-(4,4-difluorocyclohexyl)ethyl)-8-azabicyclo[3.2.1]octane-8-carboxylate (0.33 g, 93%) as a yellow gum. LCMS (method high pH): Retention time 1.68 min, $[M + H]^+$ = 712. ^{1}H NMR (400 MHz, $CDCl_3$) δ 8.49 (d, *J* = 2.0 Hz, 1H), 8.48 (d, *J* = 1.5 Hz, 1H), 7.81 (s, 1H), 7.72 (d, *J* = 1.0 Hz, 1H), 7.54 (s, 1H), 7.51−7.47 (m, 2H), 7.45−7.40 (m, 2H), 7.37−7.31 (m, 1H), 6.05 (d, *J* = 9.5 Hz, 1H), 5.51 (d, *J* = 2.4 Hz, 2H), 4.30 (br s, 3H), 2.44 (s, 3H), 2.37 (d, *J* = 0.7 Hz, 3H), 2.04−1.83 (m, 7H), 1.76−1.59 (m, 6H), 1.56 (s, 10H), 1.33−1.06 (m, 6H). Step 4: A solution of (1*S**,2*S**,3*R**,5*R**)-*tert*-butyl 3-((2-(benzyloxy)-3-methyl-5-(5-methylpyridin-3-yl)-1,7-naphthyridin-8-yl)amino)-2-(2-(4,4-difluorocyclohexyl)ethyl)-8-azabicyclo[3.2.1]octane-8-carboxylate (0.33 g, 0.46 mmol) in TFA (3 mL) was refluxed for 5 h then was cooled to room temperature and concentrated in vacuo. The residue was loaded onto a 10 g SCX2 cartridge, which was washed with MeOH (20 mL) and eluted with a 2N NH_3 solution in MeOH (20 mL). The eluant was concentrated in vacuo to give 8-(((1*S**,2*R**,3*R**,5*R**)-2-(2-(4,4-difluorocyclohexyl)ethyl)-8-azabicyclo[3.2.1]octan-3-yl)amino)-3-methyl-5-(5-methylpyridin-3-yl)-1,7-naphthyridin-2(1*H*)-one (0.18 g, 74%) as a white foam. LCMS (method high pH): Retention time 1.01 min, $[M + H]^+$ = 522. ^{1}H NMR (400 MHz, DMSO-d_6) δ 8.44 (d, *J* = 1.5 Hz, 1H), 8.37 (d, *J* = 2.0 Hz, 1H),7.69 (s, 1H), 7.61 (s, 1H), 7.51 (d, *J* = 1.2 Hz, 1H), 6.72 (d, *J* = 8.1 Hz, 1H), 4.22−4.07 (m, 1H), 3.49−3.18 (m, 5H), 2.38 (s, 3H), 2.08 (d, *J* = 1.0 Hz, 3H), 1.98−1.84 (m, 3H), 1.81−1.46 (m, 10H), 1.38−1.12 (m, 4H), 1.03−0.94 (m, 2H). Step 5: The two enantiomers of 8-(((1*S**,2*R**,3*R**,5*R**)-2-(2-(4,4-difluorocyclohexyl)ethyl)-8-azabicyclo[3.2.1]octan-3-yl)amino)-3-methyl-5-(5-methylpyridin-3-yl)-1,7-naphthyridin-2(1*H*)-one were separated by chiral chromatography. Analytical method:: Approximately 0.5 mg of racemate were dissolved in 50% EtOH in heptane (1 mL) and 20 μLwere injected onto the column. Eluant: 10% EtOH (+0.2% isopropylamine) in heptane, *f* = 1.0 mL/min, wavelength = 215 nm. Column 4.6 mm i.d. × 25 cm Chiralcel OD-H. Preparative method: Approximately 160 mg were dissolved in EtOH (3 mL) and isopropylamine (1 mL). Then 1 mL of the solution was injected onto the column. Eluant: 10% EtOH (+0.2% isopropylamine) in heptane, *f* = 30 mL/min, wavelength 215 nm. Column 30 mm × 25 cm Chiralcel OD-H. Total number of injections: 5. The fractions were collected and concentrated in vacuo to give 8-(((1*R*,2*R*,3*R*,5*S*)-2-(2-(4,4-difluorocyclohexyl)ethyl)-8-azabicyclo[3.2.1]octan-3-yl)amino)-3-methyl-5-(5-methylpyridin-3-yl)-1,7-naphthyridin-2(1*H*)-one (76 mg, 95%) as the fastest running enantiomer and 8-(((1*S*,2*S*,3*S*,5*R*)-2-(2-(4,4-difluorocyclohexyl)ethyl)-8-azabicyclo[3.2.1]octan-3-yl)-amino)-3-methyl-5-(5-methylpyridin-3-yl)-1,7-naphthyridin-2(1*H*)-one (**25**) (71 mg, 89%) as the slowest running enantiomer.

DOI: 10.1021/acs.jmedchem.8b00862
J. Med. Chem. XXXX, XXX, XXX−XXX

8-(((3*S*,4*r*,5*R*)-3,5-Dimethoxypiperidin-4-yl)amino)-3-methyl-1,7-naphthyridin-2(1*H*)-one (30). Step 1: A mixture of (3*R*,4*r*,5*S*)-*tert*-butyl 4-amino-3,5-dimethoxypiperidine-1-carboxylate (**18a**) (0.20 g, 0.77 mmol), 2-(benzyloxy)-8-chloro-3-methyl-1,7-naphthyridine (**19a**) (0.14 g, 0.49 mmol), sodium *tert*-butoxide (0.142 g, 1.48 mmol), BrettPhos (0.026 g, 0.049 mmol), and $Pd_2(dba)_3$ (0.023 g, 0.025 mmol) in THF (5 mL) was stirred at room temperature for 1 h, then at 60 °C for 2 h before being cooled to room temperature and diluted with EtOAc (20 mL). The organic phase was washed with water, dried over $MgSO_4$, and concentrated in vacuo to give (3*S*,4*r*,5*R*)-*tert*-butyl 4-((2-(benzyloxy)-3-methyl-1,7-naphthyridin-8-yl)amino)-3,5-dimethoxypiperidine-1-carboxylate, a brown residue (100 mg, 40%) as a brown oil which was used in the next step without purification. LCMS (method high pH): Retention time 1.41 min, $[M + H]^+$ = 509. Step 2: A solution of (3*S*,4*r*,5*R*)-*tert*-butyl 4-((2-(benzyloxy)-3-methyl-1,7-naphthyridin-8-yl)amino)-3,5-dimethoxypiperidine-1-carboxylate (80 mg, 0.16 mmol) in TFA (3 mL) was refluxed for 3 h then was cooled to room temperature and concentrated in vacuo. The residue was dissolved in MeOH (3 mL) and loaded onto a 5 g SCX cartridge. This was washed with MeOH (20 mL) and then eluted with a 2N NH_3 solution in MeOH (20 mL). The eluant was concentrated in vacuo to give 8-(((3*S*,4*r*,5*R*)-3,5-dimethoxypiperidin-4-yl)amino)-3-methyl-1,7-naphthyridin-2(1*H*)-one (**27**) (48 mg, 96%) as a beige solid. LCMS (method high pH): Retention time 0.60 min, $[M + H]^+$ = 319. ^{1}H NMR (400 MHz, $CDCl_3$) δ 13.3−13.0 (br s, 1H), 8.01 (d, *J* = 5.4 Hz, 1H), 7.67 (d, *J* = 1.0 Hz, 1H), 6.72 (d, *J* = 5.4 Hz, 1H), 6.45−6.28 (m, 1H), 4.59−4.43 (m, 1H), 3.48−3.35 (m, 11H), 2.74−2.61 (m, 2H), 2.39 (d, *J* = 1.0 Hz, 3H).

■ ASSOCIATED CONTENT

Supporting Information

The Supporting Information is available free of charge on the ACS Publications website at DOI: 10.1021/acs.jmedchem.8b00862.

Full ATAD2 and BRD4 BD1 assay and ChromLogD data for exemplified compounds; full assay data for BRD4 BD1 and BD2; assay data for a set of ATAD2 inhibitors at BD1 for BRD2, BRD3, BRD4, and BRDT; comparison of activities of O- and C-linked piperidine derivatives; data collection and refinement statistics for ATAD2 and BRD4 BD1 X-ray structures; OMIT maps for ATAD2 and BRD4 BD1 X-ray structures; side chain torsion angles of Trp81 in the complex with **26** compared to other structures of BRD4 BD1 from the Protein Data Bank; supplementary methods; LCMS traces (DOCX)

Molecular formula strings (CSV)

Accession Codes

PDB IDs of new crystal (X-ray) structures: 6HDN, 6HDO, and 6HDQ. Authors will release the atomic coordinates upon article publication.

■ AUTHOR INFORMATION

Corresponding Authors

*For P.B.: phone, +44 1438 763246; fax, +44 1438 763352; E-mail, Paul.A.Bamborough@gsk.com.

*For E.H.D.: phone, +44 1438 764319; fax, +44 1438 768302; E-mail, Emmanuel.H.Demont@gsk.com.

ORCID

Paul Bamborough: 0000-0001-9479-2894

Present Address

⊥For R.J.S.: Oncology Innovative Medicines and Early Development, AstraZeneca, Cambridge Science Park, Milton Road, Cambridge CB4 OWG, U.K.

Notes

The authors declare the following competing financial interest(s): All authors are current or previous employees of GSK.

■ ACKNOWLEDGMENTS

Thanks to Dr. Richard Upton for NMR support and Phylicia Dassardo Joseph and Abigail Lucas for crystallization support.

■ ABBREVIATIONS USED

ANCCA, AAA nuclear coregulator cancer-associated protein; ATAD2, ATPase family AAA domain containing 2; BET, bromodomain and extra terminal domain; BRD4/7/9, bromodomain-containing protein 4/7/9; BRPF1, bromodomain and PHD finger containing 1; CBP, CREB binding protein; CREB, cAMP response element-binding protein; EP300, histone acetyltransferase p300; KAc, acetyl lysine; pIC_{50}, $-\log_{10}$ IC_{50}; SMARCA2/4, SWI/SNF related, matrix associated, actin dependent regulator of chromatin, subfamily a, member 2/4

■ REFERENCES

(1) Morozumi, Y.; Boussouar, F.; Tan, M.; Chaikuad, A.; Jamshidikia, M.; Colak, G.; He, H.; Nie, L.; Petosa, C.; de Dieuleveult, M.; Curtet, S.; Vitte, A.-L.; Rabatel, C.; Debernardi, A.; Cosset, F.-L.; Verhoeyen, E.; Emadali, A.; Schweifer, N.; Gianni, D.; Gut, M.; Guardiola, P.; Rousseaux, S.; Gérard, M.; Knapp, S.; Zhao, Y.; Khochbin, S. Atad2 is a generalist facilitator of chromatin dynamics in embryonic stem cells. *J. Mol. Cell Biol.* **2016**, *8*, 349−362.

(2) Zou, J. X.; Revenko, A. S.; Li, L. B.; Gemo, A. T.; Chen, H. W. ANCCA, an estrogen-regulated AAA+ ATPase coactivator for ERalpha, is required for coregulator occupancy and chromatin modification. *Proc. Natl. Acad. Sci. U. S. A.* **2007**, *104*, 18067−18072.

(3) Kalashnikova, E. V.; Revenko, A. S.; Gemo, A. T.; Andrews, N. P.; Tepper, C. G.; Zou, J. X.; Cardiff, R. D.; Borowsky, A. D.; Chen, H. W. ANCCA/ATAD2 overexpression identifies breast cancer patients with poor prognosis, acting to drive proliferation and survival of triple-negative cells through control of B-Myb and EZH2. *Cancer Res.* **2010**, *70*, 9402−9412.

(4) Caron, C.; Lestrat, C.; Marsal, S.; Escoffier, E.; Curtet, S.; Virolle, V.; Barbry, P.; Debernardi, A.; Brambilla, C.; Brambilla, E.; Rousseaux, S.; Khochbin, S. Functional characterization of ATAD2 as a new cancer/testis factor and a predictor of poor prognosis in breast and lung cancers. *Oncogene* **2010**, *29*, 5171−5181.

(5) Fouret, R.; Laffaire, J.; Hofman, P.; Beau-Faller, M.; Mazieres, J.; Validire, P.; Girard, P.; Camilleri-Broet, S.; Vaylet, F.; Leroy-Ladurie, F.; Soria, J. C.; Fouret, P. A comparative and integrative approach identifies ATPase family, AAA domain containing 2 as a likely driver of cell proliferation in lung adenocarcinoma. *Clin. Cancer Res.* **2012**, *18*, 5606−5616.

(6) Wu, G.; Liu, H.; He, H.; Wang, Y.; Lu, X.; Yu, Y.; Xia, S.; Meng, X.; Liu, Y. miR-372 down-regulates the oncogene ATAD2 to influence hepatocellular carcinoma proliferation and metastasis. *BMC Cancer* **2014**, *14*, 107−118.

(7) Wu, G.; Lu, X.; Wang, Y.; He, H.; Meng, X.; Xia, S.; Zhen, K.; Liu, Y. Epigenetic high regulation of ATAD2 regulates the Hh pathway in human hepatocellular carcinoma. *Int. J. Oncol.* **2014**, *45*, 351−361.

(8) Hou, M.; Huang, R.; Song, Y.; Feng, D.; Jiang, Y.; Liu, M. ATAD2 overexpression is associated with progression and prognosis in colorectal cancer. *Jpn. J. Clin. Oncol.* **2016**, *46*, 222−227.

DOI: 10.1021/acs.jmedchem.8b00862
J. Med. Chem. XXXX, XXX, XXX−XXX

(9) Wrzeszczynski, K. O.; Varadan, V.; Byrnes, J.; Lum, E.; Kamalakaran, S.; Levine, D. A.; Dimitrova, N.; Zhang, M. Q.; Lucito, R. Identification of tumor suppressors and oncogenes from genomic and epigenetic features in ovarian cancer. *PLoS One* **2011**, *6*, e28503.
(10) Raeder, M. B.; Birkeland, E.; Trovik, J.; Krakstad, C.; Shehata, S.; Schumacher, S.; Zack, T. I.; Krohn, A.; Werner, H. M.; Moody, S. E.; Wik, E.; Stefansson, I. M.; Holst, F.; Oyan, A. M.; Tamayo, P.; Mesirov, J. P.; Kalland, K. H.; Akslen, L. A.; Simon, R.; Beroukhim, R.; Salvesen, H. B. Integrated genomic analysis of the 8q24 amplification in endometrial cancers identifies ATAD2 as essential to MYC-dependent cancers. *PLoS One* **2013**, *8*, e54873.
(11) Fellenberg, J.; Bernd, L.; Delling, G.; Witte, D.; Zahlten-Hinguranage, A. Prognostic significance of drug-regulated genes in highgrade osteosarcoma. *Mod. Pathol.* **2007**, *20*, 1085−1094.
(12) Zhang, M.; Zhang, C.; Du, W.; Yang, X.; Chen, Z. ATAD2 is overexpressed in gastric cancer and serves as an independent poor prognostic biomarker. *Clin. Transl. Oncol.* **2016**, *18*, 776−781.
(13) Zou, J. X.; Duan, Z.; Wang, J.; Sokolov, A.; Xu, J.; Chen, C. Z.; Li, J. J.; Chen, H. W. Kinesin family deregulation coordinated by bromodomain protein ANCCA and histone methyltransferase MLL for breast cancer cell growth, survival, and tamoxifen resistance. *Mol. Cancer Res.* **2014**, *12*, 539−549.
(14) Koo, S. J.; Fernández-Montalván, A. E.; Badock, V.; Ott, C. J.; Holton, S. J.; von Ahsen, O.; Toedling, J.; Vittori, S.; Bradner, J. E.; Gorjánácz, M. ATAD2 is an epigenetic reader of newly synthesized histone marks during DNA replication. *Oncotarget* **2016**, *7*, 70323−70335.
(15) Revenko, A. S.; Kalashnikova, E. V.; Gemo, A. T.; Zou, J. X.; Chen, H. W. Chromatin loading of E2F-MLL complex by cancer-associated coregulator ANCCA via reading a specific histone mark. *Mol. Cell. Biol.* **2010**, *30*, 5260−5272.
(16) Zou, J. X.; Guo, L.; Revenko, A. S.; Tepper, C. G.; Gemo, A. T.; Kung, H. J.; Chen, H. W. Androgen-induced coactivator ANCCA mediates specific androgen receptor signalling in prostate cancer. *Cancer Res.* **2009**, *69*, 3339−3346.
(17) Hsia, E. Y.; Kalashnikova, E. V.; Revenko, A. S.; Zou, J. X.; Borowsky, A. D.; Chen, H. W. Deregulated E2F and the AAA+ coregulator ANCCA drive proto-oncogene ACTR/AIB1 overexpression in breast cancer. *Mol. Cancer Res.* **2010**, *8*, 183−193.
(18) Duan, Z.; Zou, J. X.; Yang, P.; Wang, Y.; Borowsky, A. D.; Gao, A. C.; Chen, H. W. Developmental and androgenic regulation of chromatin regulators EZH2 and ANCCA/ATAD2 in the prostate via MLL histone methylase complex. *Prostate* **2013**, *73*, 455−466.
(19) Altintas, D. M.; Shukla, M. S.; Goutte-Gattat, D.; Angelov, D.; Rouault, J. P.; Dimitrov, S.; Samarut, J. Direct cooperation between androgen receptor and E2F1 reveals a common regulation mechanism for androgen-responsive genes in prostate cells. *Mol. Endocrinol.* **2012**, *26*, 1531−1541.
(20) Ciro, M.; Prosperini, E.; Quarto, M.; Grazini, U.; Walfridsson, J.; McBlane, F.; Nucifero, P.; Pacchiana, G.; Capra, M.; Christensen, J.; Helin, K. ATAD2 is a novel cofactor for MYC, overexpressed and amplified in aggressive tumors. *Cancer Res.* **2009**, *69*, 8491−8498.
(21) Mjelle, R.; Hegre, S. A.; Aas, P. A.; Drablos, F.; Slupphaug, G.; Saetrom, P.; Krokan, H. E. Cell cycle regulation of human DNA repair and chromatin remodeling genes. *DNA Repair* **2015**, *30*, 53−67.
(22) Koo, S. J.; Fernandez-Montalvan, A. E.; Badock, V.; Ott, C. J.; Holton, S. J.; von Ahsen, O.; Toedling, J.; Vittori, S.; Bradner, J. E.; Gorjanacz, M. ATAD2 is an epigenetic reader of newly synthesized histone marks during DNA replication. *Oncotarget* **2016**, *7*, 70323−70335.
(23) Zou, J. X.; Duan, Z.; Wang, J.; Sokolov, A.; Xu, J.; Chen, C. Z.; Li, J. J.; Chen, H. W. Kinesin family deregulation coordinated by bromodomain protein ANCCA and histone methyltransferase MLL for breast cancer cell growth, survival, and tamoxifen resistance. *Mol. Cancer Res.* **2014**, *12*, 539−549.
(24) Boussouar, F.; Jamshidikia, M.; Morozumi, Y.; Rousseaux, S.; Khochbin, S. Malignant genome reprogramming by ATAD2. *Biochim. Biophys. Acta, Gene Regul. Mech.* **2013**, *1829*, 1010−1014.
(25) Hussain, M.; Zhou, Y.; Song, Y.; Hameed, H. M. A.; Jiang, H.; Tu, Y.; Zhang, J. ATAD2 in cancer: a pharmacologically challenging but tractable target. *Expert Opin. Ther. Targets* **2018**, *22*, 85−96.
(26) Filippakopoulos, P.; Qi, J.; Picaud, S.; Shen, Y.; Smith, W. B.; Fedorov, O.; Morse, E. M.; Keates, T.; Hickman, T. T.; Felletar, I.; Philpott, M.; Munro, S.; McKeown, M. R.; Wang, Y.; Christie, A. L.; West, N.; Cameron, M. J.; Schwartz, B.; Heightman, T. D.; La Thangue, N.; French, C. A.; Wiest, O.; Kung, A. L.; Knapp, S.; Bradner, J. E. Selective inhibition of BET bromodomains. *Nature* **2010**, *468*, 1067−1073.
(27) Nicodeme, E.; Jeffrey, K. L.; Schaefer, U.; Beinke, S.; Dewell, S.; Chung, C.-w.; Chandwani, R.; Marazzi, I.; Wilson, P.; Coste, H.; White, J.; Kirilovsky, J.; Rice, C. M.; Lora, J. M.; Prinjha, R. K.; Lee, K.; Tarakhovsky, A. Suppression of inflammation by a synthetic histone mimic. *Nature* **2010**, *468*, 1119−1123.
(28) Filippakopoulos, P.; Knapp, S. Targeting bromodomains: epigenetic readers of lysine acetylation. *Nat. Rev. Drug Discovery* **2014**, *13*, 337−356.
(29) Theodoulou, N. H.; Tomkinson, N. C.; Prinjha, R. K.; Humphreys, P. G. Clinical progress and pharmacology of small molecule bromodomain inhibitors. *Curr. Opin. Chem. Biol.* **2016**, *33*, 58−66.
(30) Theodoulou, N. H.; Tomkinson, N. C. O.; Prinjha, R. K.; Humphreys, P. G. Progress in the development of non-BET bromodomain chemical probes. *ChemMedChem* **2016**, *11*, 477−487.
(31) Moustakim, M.; Clark, P. G. K.; Hay, D. A.; Dixon, D. J.; Brennan, P. E. Chemical probes and inhibitors of bromodomains outside the BET family. *MedChemComm* **2016**, *7*, 2246−2264.
(32) Romero, F. A.; Taylor, A. M.; Crawford, T. D.; Tsui, V.; Cote, A.; Magnuson, S. Disrupting acetyl-lisine recognition: progress in the development of bromodomain inhibitors. *J. Med. Chem.* **2016**, *59*, 1271−1298.
(33) Muller, S.; Knapp, S. Discovery of BET bromodomain inhibitors and their role in target validation. *MedChemComm* **2014**, *5*, 288−296.
(34) Demont, E. H.; Chung, C.-W.; Furze, R. C.; Grandi, P.; Michon, A.-M.; Wellaway, C.; Barrett, N.; Bridges, A. M.; Craggs, P. D.; Diallo, H.; Dixon, D. P.; Douault, C.; Emmons, A. J.; Jones, E. J.; Karamshi, B.; Locke, K.; Mitchell, D. J.; Mouzon, B. H.; Prinjha, R. K.; Roberts, A. D.; Sheppard, R. J.; Watson, R. J.; Bamborough, P. Fragment-based discovery of low-micromolar ATAD2 bromodomain inhibitors. *J. Med. Chem.* **2015**, *58*, 5649−5673.
(35) Bamborough, P.; Chung, C.-W; Furze, R. C.; Grandi, P.; Michon, A.-M.; Sheppard, R. J.; Barnett, H.; Diallo, H.; Dixon, D. P.; Douault, C.; Jones, E. J.; Karamshi, B.; Mitchell, D. J.; Prinjha, R. K.; Rau, C.; Watson, R. J.; Werner, T.; Demont, E. H. Structure-based optimization of naphthyridones into potent ATAD2 bromodomain inhibitors. *J. Med. Chem.* **2015**, *58*, 6151−6178.
(36) Miller, D. C.; Martin, M. P.; Adhikari, S.; Brennan, A.; Endicott, J. A.; Golding, B. T.; Hardcastle, I. R.; Heptinstall, A.; Hobson, S.; Jennings, C.; Molyneux, L.; Ng, Y.; Wedge, S. R.; Noble, M. E. M.; Cano, C. Identification of a novel ligand for the ATAD2 bromodomain with selectivity over BRD4 through a fragment growing approach. *Org. Biomol. Chem.* **2018**, *16*, 1843−1850.
(37) Fernandez-Montalvan, A. E.; Berger, M.; Kuropka, B.; Koo, S. J.; Badock, V.; Weiske, J.; Puetter, V.; Holton, S. J.; Stöckigt, D.; ter Laak, A.; Centrella, P. A.; Clark, M. A.; Dumelin, C. E.; Sigel, E. A.; Soutter, H. H.; Troast, D. M.; Zhang, Y.; Cuozzo, J. W.; Keefe, A. D.; Roche, D.; Rodeschini, V.; Chaikuad, A.; Diaz-Sáez, L.; Bennett, J. M.; Fedorov, O.; Huber, K. V. M; Hubner, J.; Weinmann, H.; Hartung, I. V.; Gorjánácz, M. Isoform-selective ATAD2 chemical probe with novel chemical structure and unusual mode of action. *ACS Chem. Biol.* **2017**, *12* (12), 2730−2736.
(38) Harner, M. J.; Chauder, B. A.; Phan, J.; Fesik, S. W. Fragment-based screening of the bromodomain of ATAD2. *J. Med. Chem.* **2014**, *57*, 9687−9692.
(39) Bamborough, P.; Chung, C.-W; Demont, E. H.; Furze, R. C.; Bannister, A. J.; Che, K. H.; Diallo, H.; Douault, C.; Grandi, P.; Kouzarides, T.; Michon, A.-M.; Mitchell, D. J.; Prinjha, R. K.; Rau, C.;

DOI: 10.1021/acs.jmedchem.8b00862
J. Med. Chem. XXXX, XXX, XXX−XXX

Robson, S.; Sheppard, R. J.; Upton, R.; Watson, R. J. A chemical probe for the ATAD2 bromodomain. *Angew. Chem., Int. Ed.* **2016**, *55*, 11382−11386.
(40) GSK8814 is available via the Structural Genomic Consortium: http://www.thesgc.org/ (accessed June 28, 2018).

DOI: 10.1021/acs.jmedchem.8b00862
J. Med. Chem. XXXX, XXX, XXX−XXX